ARR No. L4I11e

NATIONAL ADVISORY COMMITTEE FOR AERONAUTICS

WARTIME REPORT

ORIGINALLY ISSUED
September 1944 as
Advance Restricted Report L4I11e

HIGH-ALTITUDE COOLING

VI - AXIAL-FLOW FANS AND COOLING POWER

By William Mutterperl

Langley Memorial Aeronautical Laboratory
Langley Field, Va.

NACA

WASHINGTON

NACA ARR No. L4I11e

NATIONAL ADVISORY COMMITTEE FOR AERONAUTICS

ADVANCE RESTRICTED REPORT

HIGH-ALTITUDE COOLING

VI - AXIAL-FLOW FANS AND COOLING POWER

By William Mutterperl

SUMMARY

The theory, design, and effect on cooling of the constant-velocity axial-flow fan as related to the problem of high-altitude aircraft engine cooling are discussed in the present report. The existing theory of the axial-flow fan, including a discussion of the fan losses, is summarized. Nondimensional design and performance formulas are developed for stator-rotor, rotor-stator, and rotor-alone fan combinations. Charts based on these formulas are given to facilitate performance estimates and design. Some illustrative fan designs are made for an altitude of 40,000 feet. Finally, the effect of a fan on cooling power is quantitatively discussed and illustrated.

The results of the present study indicate that an axial-flow fan may be used to give a moderate pressure rise to a large flow quantity of air; that existing theory provides a satisfactory basis for the design of axial-flow fans; that the use of stationary guide vanes and small rotor tip clearances is essential for efficient fan design; that further research is needed for the development of airfoil sections especially suitable for use in high-speed, high-solidity rotors; that the losses in internal cooling power at high altitude are large when the cooling is marginal; and that an axial-flow fan more than pays for itself in cooling power saved when cooling conditions are marginal.

INTRODUCTION

As part of a general study of various aspects of the problem of high-altitude engine cooling (see reference 1), the theory, design, and effect on cooling of the constant-velocity axial-flow fan are considered in the present report.

An axial-flow fan may be effectively used as an engine-cooling aid at high altitude, where the necessary cooling pressure is not entirely available or where, if obtainable with large exit flaps and flap deflections, the resulting drag would be prohibitive. Although the fan itself acts primarily to increase the pressure of the air passing through it, several other beneficial effects result from its use in an airplane.

First, the pressure increase of the cooling air allows a decrease in the ultimate kinetic energy of the cooling air following the airplane. The net power saved in this way may be more than the power required to drive the fan, with a resulting increase in propulsive efficiency for the airplane as a whole. This effect will be discussed quantitatively in a later section.

Furthermore, an axial-flow fan mounted at the entrance of a cowling can decrease the lower limit of cowling inlet velocity for smooth-entry flow and improve the axial velocity distribution around the inside of the cowling. The reason probably lies in the fact that the pressure rise across a fan goes up if the flow through it goes down and vice versa; hence, any variations in the axial velocity distribution in front of the fan produced by boundary layers or by the attitude of the airplane tend to be ironed out by suitable pressure gradients produced by the fan. It may also be mentioned that a fan at the entrance of a cowling is subject to the same angle-of-attack effects as a propeller; that is, if the fan axis is tilted upward relative to the incoming flow, the blades on the downgoing side are more highly loaded, and hence produce a higher pressure rise, than the blades on the upgoing side.

The design of an axial-flow fan must be carried out with the characteristics of its power supply in mind. There are three primary sources of power on an airplane in flight; namely, the engine, the engine exhaust gases, and the motion of the airplane relative to the air. The corresponding devices for transferring this power to the fan would be a gear or direct drive from the engine, an exhaust-gas turbine, and a windmill. Each device can be used practicably to drive the fan and the choice therefore depends on considerations of engine and cowling design.

The theory of the constant-velocity axial-flow fan operating in an incompressible fluid, together with design formulas and charts, is presented in the sections immediately following. The design procedure as well as the cooling possibilities at altitude of the axial-flow fan is then illustrated by the design of three arrangements of single-stage axial-flow fan for operation at 40,000 feet. The concluding section deals with the internal-power losses in a cooling installation, with compressibility effects included.

SYMBOLS

q	dynamic pressure $\left(\frac{1}{2}\rho V^2\right)$
p	static pressure
Δp	change of static pressure
V	velocity
V_o	free-stream velocity
ρ	density
G	mass flow per unit area (ρV)
Q	quantity rate of flow
M	mass rate of flow
H	heat rate of flow
P	power
η	efficiency
s	cascade spacing
w	relative velocity
X	x-direction (tangential) force per blade per unit span
Y	y-direction (axial) force per blade per unit span
l	"lift" per blade per unit span
d	drag per blade per unit span
Γ	circulation
c	blade chord
c_l	section lift coefficient
c_d	section drag coefficient
c_p	section pressure coefficient; also, specific heat at constant pressure

c_v specific heat at constant volume

c_T section torque coefficient

r radial location of blade element

x nondimensional blade-element radial location (r/R_o)

R_o fan radius at outer section

R_h fan radius at hub section

ω angular velocity

u velocity in rotational direction

n rotational speed, revolutions per unit time

B number of blades

N rotation parameter $(\omega r/V_f)$

γ circulation parameter (Γ/cV_f); also, ratio of specific heats (c_p/c_v)

σ solidity $(Bc/2\pi r)$

T torque; also, temperature

T_w average cooler temperature

α angle of attack

β blade angle measured from zero lift line to fan plane

β' blade angle measured from chord line to fan plane

ϕ relative stream angle measured from relative velocity direction to fan plane

f Collar cascade lift factor

δ Ruden cascade thickness correction

S blade profile area

D diameter; also, reciprocal of profile aspect ratio (S/c^2)

a_o slope of section lift curve

α_{l_o} angle of attack for zero lift

A cross-sectional area

a speed of sound

Subscripts:

f fan

h hub section

r cooling resistance; also, rotor

o output; also, outer

l total loss

i ideal; also, inlet

d diffuser; also, drag

m momentum

p pressure

x x direction

y y direction

1 entrance

f1 upstream of fan

f2 downstream of fan

2 cooling-resistance entrance

3 downstream of cooling resistance

3e cooling-resistance exit

4 ultimate exit condition

s stator; also, stagnation

t tip clearance

max maximum

THEORY OF THE AXIAL-FLOW FAN

The axial-flow fan consists essentially of one or more sets of rotating impeller vanes, hereinafter called "rotors," which may be operated in conjunction with one or more sets of stationary guide vanes, hereinafter called "stators." (See fig. 1.) A rotor operating alone increases the static pressure and puts kinetic energy of rotation into the fluid passing through it in the axial direction. A stator may be used behind or downstream of the rotor to convert the kinetic energy of rotation into additional static-pressure increase. There is then a static-pressure rise across both rotor and stator. A stator may, on the other hand, be placed ahead or upstream of the rotor as in figure 1. In this case the stator twists and reduces the static pressure of the flow, which is then straightened and increased in pressure by the rotor.

The analysis of the axial-flow fan can be greatly simplified if three effects are neglected. The first is concerned with the various boundary-layer motions, the so-called secondary flows, which arise in response to the pressure gradients set up by the fan operation. So far only a qualitative insight into these phenomena has been gained. (See reference 2, sec. V.) The second effect is that of the radial velocities produced by nonuniformity of pressure increase over the fan area. Ruden (reference 2) has investigated this effect and gives a method of averaging the fan blade-element characteristics calculated for zero radial velocities for the determination of the over-all fan characteristics. At the design operating point the design criterion is uniform total pressure, with the result that radial velocity components and a nonuniform energy distribution in the flow through the fan do not arise. Radial velocities may therefore be neglected if the design operating conditions are adhered to. For other operating conditions, at which radial velocities may not be negligible, the averaging method of reference 2 can be used. Finally, the spanwise mutual interference of the blade elements is neglected. This assumption is well justified when the blade circulation is constant along the span (the design condition) or when the number of blades is large, as in an axial fan designed for high pressure rise.

Consider the annular area of a set of blades (fig. 2) included between the radial stations r and $r + dr$ and rotating with angular velocity ω in a flow that has both an axial velocity component V_f and an initial rotational velocity component u_1. Positive directions are indicated by the arrows in the figure. Under the assumptions made, the annular set of blades may be regarded as a two-dimensional cascade of airfoils. It is desired to express the forces on an airfoil of the cascade in terms of a lift and drag force analogous, if possible, to the forces on an isolated airfoil. To this end the cascade is regarded as stationary, its original velocity ωr being imparted in reverse to the fluid. The equation of continuity, Bernoulli's theorem, and the momentum theorem are then applied to the fluid within the boundary ABCDEF where ABC and FED are relative streamlines and AF and CD are sections 1 and 2 parallel to the cascade direction. Drag effects are for the moment neglected, with the result that the flow is uniform at the sections 1 and 2.

The equation of continuity is simply

$$V_f = \text{Constant} \tag{1}$$

Bernoulli's theorem for sections 1 and 2 is

$$p_1 + \frac{1}{2}\rho\left[V_f^2 + (\omega r + u_1)^2\right] = p_2 + \frac{1}{2}\rho\left[V_f^2 + (\omega r + u_2)^2\right] \tag{2}$$

The momentum theorem gives the force components X and Y on the blade element per unit length of blade span. If it is remembered that the pressures at similar points on the streamlines ABC and FED are the same and if the continuity condition of equation (1) is used, then the momentum equations are

$$\left.\begin{aligned} &\text{x direction (tangential)} \\ &X = \rho s V_f(u_1 - u_2) \\ &\text{y direction (axial)} \\ &Y = s(p_1 - p_2) \end{aligned}\right\} \tag{3}$$

or, using Bernoulli's equation (2),

$$Y = \rho s\left(u_2 - u_1\right)\left(\omega r + \frac{u_1 + u_2}{2}\right) \tag{4}$$

The forces X and Y are the components of a "lift" per unit span

$$l = \rho w \Gamma \tag{5}$$

where

$$\Gamma = s(u_1 - u_2) \tag{6}$$

and

$$w = \sqrt{V_f^2 + \left(\omega r + u_1 - \frac{B\Gamma}{4\pi r}\right)^2} \tag{7}$$

The cascade spacing s of equations (3) and (4) has been expressed in equation (7) in terms of the circumference and number of blades

$$s = \frac{2\pi r}{B}$$

The quantity Γ defined by equation (6) is the circulation around the blade element. The velocity w is the mean of the relative velocities upstream and downstream of the annulus. For large values of the ratio of blade spacing to blade chord s/c, the velocity w approximates the actual flow in which the blade element acts. The lift l on the blade element acts at right angles to the mean relative velocity w, in analogy with the lift on an isolated airfoil. In addition to the lift there is a profile drag d, which is customarily assumed to act in the direction of w whereas its magnitude must be given by experiment. Although this assumption is in error, as discussed in the section "Fan Losses," it will be at least temporarily retained because of its simplicity and because the over-all error is not large.

With the aid of equations (5) and (2), the lift, the drag, and the mean relative velocity can be expressed nondimensionally. If c is the local blade chord,

$$c_l \equiv \frac{l}{\frac{1}{2}\rho w^2 c} = \frac{2\gamma}{w/V_f} \tag{8}$$

$$c_d \equiv \frac{d}{\frac{1}{2}\rho w^2 c} \tag{9}$$

$$\frac{w}{V_f} = \frac{1}{\sin \phi} = \sqrt{1 + \left(N + \frac{u_1}{V_f} - \frac{\gamma\sigma}{2} \right)^2} \tag{10}$$

where

the rotation parameter

$$N = \frac{\omega r}{V_f}$$

the circulation parameter

$$\gamma = \frac{\Gamma}{cV_f}$$

the solidity

$$\sigma = \frac{Bc}{2\pi r}$$

and the mean relative stream angle ϕ is shown in figure 2. The pressure rise Δp and the torque T per unit length spanwise of the rotor are obtained by resolving these forces parallel and perpendicular to the fan axis. The nondimensional results are

$$c_p = \frac{\Delta p_f}{q_f}$$

$$= 2\gamma\sigma\left(N + \frac{u_1}{V_f} - \frac{\gamma\sigma}{2} \right) - \sigma c_d \frac{w}{V_f} \tag{11}$$

$$c_T = \frac{T}{2\pi r^2 q_f}$$

$$= 2\gamma\sigma + \sigma c_d \frac{w}{V_f}\left(N + \frac{u_1}{V_f} - \frac{\gamma\sigma}{2} \right) \tag{12}$$

The power output dP_o of the annulus is $dQ\Delta p$ where

$$dQ = 2\pi r V_f dr$$

Thus,

$$dP_o = 2\pi r V_f \Delta p_f dr \tag{13}$$

and the power input to the annulus is

$$dP_i = T\omega\, dr \tag{14}$$

which gives a section efficiency of

$$\eta = \frac{c_p}{Nc_T} \tag{15}$$

These quantities, as well as the pressure and torque, may be suitably integrated over the fan area; but due account should be taken of the tip-clearance losses discussed later.

By using equations (8) and (10) the circulation parameter γ can be eliminated from equations (11) and (12), giving the pressure and torque in terms of known quantities and the lift and drag coefficients of the blade element. The problem thus resolves itself into the determination of the angle of attack α of the blade element relative to the mean flow w to give a lift coefficient c_l and the determination of the corresponding drag coefficient c_d. Before these questions are taken up, the fan losses will be discussed and the performance formulas of various combinations of rotor and stator derived.

FAN LOSSES

Three main energy losses and one potential source of energy loss arise in the action of a rotor: (1) the profile-drag losses on the blades, (2) the tip-clearance losses, (3) the inner-wall losses, and (4) the rotational kinetic energy of the flow downstream of the rotor.

(1) The profile drag of the blade element has been approximately taken into account by a drag at right angles to the lift. A more detailed analysis of a cascade, similar to that previously given for the frictionless case but including the effect of a wake that starts from the trailing edge of each airfoil and passes downstream with gradually increasing thickness, shows that equations (1) and (2) must be altered. If the subscript 2 denotes the ultimate downstream condition in which complete mixing of the wake has occurred, then equation (2) for the pressure rise has an additional, essentially positive term on the right-hand side. This term is a function of the velocities and dimensions of the wake at an arbitrary downstream location, and equation (2) shows that it is invariant with respect to distance downstream from the cascade. It

represents a drag in the axial direction. The lift, acting perpendicular to the mean flow, is still given by equations (5) to (7) but, as noted, with the subscript 2 referring to ultimate downstream conditions.

The resultant force on an airfoil in a cascade may of course be resolved, although somewhat artificially in view of the preceding remarks, into components in any direction. It was found in reference 3 that, for a typical rotor blade, the profile-drag coefficient in the mean-flow direction was greater than the isolated section value by about 30 percent, and this fact will be used in the section "Illustrative Fan Designs." It seems, however, that drag measurements on airfoils in cascade should be presented in terms of a more rigorous analysis such as just indicated.

(2) The tip-clearance losses are usually much greater than the profile-drag losses. They are caused by flow leakage from the high-pressure to the low-pressure side around the blade tip. The loss in efficiency due to tip clearance is evidenced as a reduction in pressure rise of the fan, the power taken by the fan remaining about the same for all clearances. This effect is probably largely caused by turbulent mixing in the axial direction.

In reference 2, the tip-clearance losses were determined experimentally for an eight-blade rotor-stator combination with rotor solidity σ varying from 0.79 at the hub to 0.52 at the tip section. The hub diameter was 9.85 inches and the outer-wall diameter was 19.7 inches. Figure 3 presents the mean of curves determined for three different blade loadings. The separate curves depart from the mean by about 1 percent. The reduction in pressure due to tip clearance is large, about 7.5 percent for a clearance of only 2 percent of the blade span.

(3) The inner-wall losses are caused by the boundary layer on the inner wall of the rotor. By the same argument as previously given these losses should also manifest themselves as a reduction in pressure rise. The dead air at the hub, however, is swept to the tip by the centrifugal force of rotor rotation, with the result that these losses may be largely included in the tip-clearance losses. Some measurements of wall losses in a stationary cascade are given in reference 4. The results are not directly applicable to a rotor, however, because of the spanwise flow of dead air just mentioned.

(4) The rotational kinetic energy of the downstream flow represents a loss if it is not transformed to pressure energy by a set of stationary guide vanes or by other means. This loss represents a drop in pressure rise and is included in equation (11) for c_p.

PERFORMANCE FORMULAS FOR VARIOUS FAN COMBINATIONS

Stator Upstream of Rotor

The arrangement in which the stator is upstream of the rotor will be referred to as a "stator-rotor combination." Subscript s will designate stator quantities; r, rotor quantities.

The initial flow into the stator is assumed to have no rotational component, that is, $u_1 = 0$ for the stator. The flow emerging from the stator will have a rotational velocity component $\gamma_s \sigma_s V_f$ that is to cancel the rotational velocity component $\gamma_r \sigma_r V_f$ of the rotor. The product $\gamma\sigma$ (no subscripts are necessary) is therefore the same for rotor and stator at any radial location; hence, for the stator the relative velocity w_s/V_f is, from equation (10),

$$\frac{w_s}{V_f} = \sqrt{1 + \left(\frac{\gamma\sigma}{2}\right)^2} \tag{16}$$

and the lift coefficient is given by

$$\sigma_s c_{l_s} = \frac{2\gamma\sigma}{w_s/V_f}$$

The pressure rise, which is negative, is, from equation (11),

$$c_{p_s} = \frac{\Delta p_{f_s}}{q_f}$$

$$= -(\gamma\sigma)^2 - \sigma_s c_{d_s} \frac{w_s}{V_f} \tag{17}$$

For the rotor, if it is remembered that $\frac{u_1}{V_f} = \gamma\sigma$ and if the small effect of the stator drag on the momentum change through the stator is neglected, there is obtained from equations (8) and (10) to (12)

$$\frac{w_r}{V_f} = \frac{1}{\sin \phi_r}$$

$$= \sqrt{1 + \left(N + \frac{\gamma\sigma}{2}\right)^2} \tag{18}$$

$$c_{p_r} = \frac{\Delta p_{f_r}}{q_f}$$

$$= 2\gamma\sigma N + (\gamma\sigma)^2 - \sigma_r c_{d_r} \frac{w_r}{V_f} \tag{19}$$

$$c_T = \frac{T}{2\pi r^2 q_f}$$

$$= 2\gamma\sigma + \sigma_r c_{d_r} \frac{w_r}{V_f}\left(N + \frac{\gamma\sigma}{2}\right) \tag{20}$$

$$\sigma_r c_{l_r} = \frac{\sigma_r l_r}{\frac{1}{2}\rho w_r^2 c_r}$$

$$= \frac{2\gamma\sigma}{w_r/V_f} \tag{21}$$

The pressure rise for the stage is the sum of equations (17) and (19) minus the loss due to tip clearance c_{p_t}:

$$c_{p_f} = \frac{\Delta p_f}{q_f}$$

$$= 2\gamma\sigma N - \sigma_r c_{d_r} \frac{w_r}{V_f} - \sigma_s c_{d_s} \frac{w_s}{V_f} - c_{p_t} \tag{22}$$

A relatively simple expression for the pressure rise in terms of the rotor lift coefficient can be obtained by neglecting the drag and the tip-clearance terms in equation (22), which may be corrected for afterward, and combining the result with equation (21) to eliminate $\gamma\sigma$. The result is

$$\sigma_r c_{l_r} = \frac{c_{p_{f_i}}}{N\sqrt{1 + \left(N + \frac{c_{p_{f_i}}}{4N}\right)^2}}$$

or

$$c_{p_{f_i}} = \frac{1 + \sqrt{1 + \left(\frac{1}{N^2} + 1\right)\left(\frac{16}{\sigma^2 c_l{}^2} - 1\right)}}{\frac{1}{4N^2}\left(\frac{16}{\sigma^2 c_l{}^2} - 1\right)} \qquad (23)$$

where

$$c_{p_{f_i}} = \left(\frac{\Delta p_f}{q_f}\right)_{ideal}$$

$$= 2\gamma\sigma N$$

Equations (18) and (20) can now be rewritten in terms of the ideal pressure rise

$$\frac{w_r}{V_f} = \frac{1}{\sin \phi_r}$$

$$= \sqrt{1 + \left(N + \frac{c_{p_{f_i}}}{4N}\right)^2} \qquad (24)$$

$$c_T = \frac{T}{2\pi r^2 q_f}$$

$$= \frac{c_{p_{f_i}}}{N} + \sigma_r c_{d_r} \frac{w_r}{V_f}\left(N + \frac{c_{p_{f_i}}}{4N}\right)$$

The expressions (23) and (24) suffice to determine the rotor blade-element lift coefficient and the relative stream angle at any radial location from a desired "frictionless" pressure rise $(\Delta p_f/q_f)_{ideal}$. Both of these formulas are illustrated graphically in figures 4 and 5.

Figure 4(a) is based on equation (23) and gives $c_{p_{f_i}}$ against N with $\sigma_r c_{l_r}$ as parameter. Figure 5(a) is based on equation (24) and gives $c_{p_{f_i}}$ against N with w_r/V_f or the corresponding ϕ_r as parameter. Figures 4(b) and 5(b) extend the range of the charts to high values of N. For convenience, pressure rise is given in terms of the related coefficient

$$c_{p_{f_i}}' = \left(\frac{\Delta p_f}{\rho n^2 D^2}\right)_{ideal}$$

where

$$c_{p_{f_i}}' = \frac{\pi^2 c_{p_{f_i}}}{2N^2}$$

This relation is plotted in figure 4(b). These charts are useful in making quick estimates of fan performance at various design operating conditions as well as in actual blade design.

For example, suppose the speed of rotation and axial velocity of flow are such that $N = \frac{w_r}{V_f} = 1$ for a rotor blade element in a stator-rotor arrangement. If the blade element is operating at a lift coefficient of 0.7 and the annulus is of solidity 0.8, then $\sigma c_l = 0.56$ and figure 4(a) gives $(\Delta p_f/q_f)_{ideal} = 0.87$. If an efficiency of 85 percent is assumed to apply to the pressure, then $\frac{\Delta p_f}{q_f} = 0.87 \times 0.85 = 0.74$. Figure 5(a) gives the mean relative stream angle ϕ_r. For $N = 1$ and $(\Delta p_f/q_f)_{ideal} = 0.87$, $\phi_r = 39.5^\circ$. The blade element should therefore be set sufficiently in excess of 39.5° to operate at a lift coefficient of 0.7. (See section "Airfoil Characteristics for Cascade Operation.")

At the design point the rise in total pressure (in this case, static pressure) is to be constant over the blower plane. Inasmuch as the profile-drag terms will not vary much over the blade span, the design criterion is taken to be

$$c_{p_{f_i}} = 2\gamma\sigma N = \frac{B\Gamma\omega}{\pi V_f^2} = \text{Constant} \qquad (25)$$

The blade circulation on both stator and rotor will therefore be constant along the span.

Rotor Upstream of Stator

The arrangement in which the rotor is upstream of the stator will be referred to as a "rotor-stator combination."

The initial flow into the rotor is assumed to have no rotational component, that is, $u_1 = 0$ for the rotor. Also, the rotational component produced by the rotor is to be completely canceled by the stator and, again,

$$\gamma_r \sigma_r = \gamma_s \sigma_s = \gamma\sigma$$

The only difference between the formulas for this case and for the stator-rotor combination is produced by a difference in the sign of the stator circulation. Thus, for the rotor,

$$\frac{w_r}{V_f} = \frac{1}{\sin \phi_r}$$

$$= \sqrt{1 + \left(N - \frac{\gamma\sigma}{2}\right)^2} \tag{26}$$

$$c_{p_r} = \frac{\Delta p_{f_r}}{q_f}$$

$$= 2\gamma\sigma N - (\gamma\sigma)^2 - \sigma_r c_{d_r} \frac{w_r}{V_f} \tag{27}$$

$$c_T = \frac{T}{2\pi r^2 q_f}$$

$$= 2\gamma\sigma + \sigma_r c_{d_r} \frac{w_r}{V_f}\left(N - \frac{\gamma\sigma}{2}\right) \tag{28}$$

$$\sigma_r c_{l_r} = \frac{\sigma_r l_r}{\frac{1}{2}\rho w_r^2 c_r}$$

$$= \frac{2\gamma\sigma}{w_r/V_f}$$

For the stator

$$\frac{w_s}{V_f} = \sqrt{1 + \left(\frac{\gamma\sigma}{2}\right)^2}$$

$$\sigma_s c_{l_s} = \frac{2\gamma\sigma}{w_s/V_f}$$

and the pressure rise

$$c_{p_s} = (\gamma\sigma)^2 - \sigma_s c_{d_s} \frac{w_s}{V_f} \tag{29}$$

The over-all pressure rise for the stage, including the tip-clearance losses c_{p_t}, is

$$c_{p_f} = \frac{\Delta p_f}{q_f}$$

$$= 2\gamma\sigma N - \sigma_r c_{d_r} \frac{w_r}{V_f} - \sigma_s c_{d_s} \frac{w_s}{V_f} - c_{p_t} \tag{30}$$

which is the same in form as the corresponding expression for the stator-rotor combination. If the friction terms in equation (30) are neglected, the frictionless pressure rise may again be expressed in terms of the rotor lift coefficient

$$\left.\begin{aligned} \sigma_r c_{l_r} &= \frac{c_{p_{f_i}}}{N\sqrt{1+\left(N-\frac{c_{p_{f_i}}}{4N}\right)^2}} \\ c_{p_{f_i}} &= \frac{-1+\sqrt{1+\left(\frac{1}{N^2}+1\right)\left(\frac{16}{\sigma^2 c_l{}^2}-1\right)}}{\frac{1}{4N^2}\left(\frac{16}{\sigma^2 c_l{}^2}-1\right)} \end{aligned}\right\} \qquad (31)$$

and, if equations (26) and (28) are rewritten in terms of the frictionless pressure rise,

$$\begin{aligned} \frac{w_r}{V_f} &= \frac{1}{\sin \phi_r} \\ &= \sqrt{1+\left(N-\frac{c_{p_{f_i}}}{4N}\right)^2} \end{aligned} \qquad (32)$$

$$\begin{aligned} c_T &= \frac{T}{2\pi r^2 q_f} \\ &= \frac{c_{p_{f_i}}}{N} + \sigma_r c_{d_r} \frac{w_r}{V_f}\left(N-\frac{c_{p_{f_i}}}{4N}\right) \end{aligned}$$

Equations (31) and (32) are the basis of the design charts given in figures 6 and 7. For the data of the stator-rotor example, that is, $N = 1$ and $\sigma c_l = 0.56$, figure 6(a) gives $(\Delta p_f/q_f)_{ideal} = 0.72$ and figure 7(a) gives a mean relative stream angle of 50.6°. For a fan efficiency of 0.85, $\Delta p_f/q_f = 0.61$ in comparison with $\Delta p_f/q_f = 0.74$ for the stator-rotor arrangement.

Rotor Alone

The initial flow is assumed to have no rotation. The formulas for the rotor alone are the same as the rotor formulas (25) to (28) pertaining to the rotor-stator combination, except that equation (27) for the pressure rise must be rewritten to include the clearance losses

$$c_{p_f} = \frac{\Delta p_f}{q_f}$$

$$= 2\gamma\sigma N - (\gamma\sigma)^2 - \sigma c_d \frac{w}{V_f} - c_{p_t} \qquad (33)$$

or, in terms of the frictionless pressure rise,

$$c_{p_f} = c_{p_{f_i}} - \left(\frac{c_{p_{f_i}}}{2N}\right)^2 - \sigma c_d \frac{w}{V_f} - c_{p_t}$$

Figures 6 and 7 can also be used in this case if the frictionless pressure $c_{p_{f_i}}$ of the figures is reduced by the rotational loss $(\gamma\sigma)^2 = \left(c_{p_{f_i}}/2N\right)^2$ in addition to the friction terms to get the actual pressure rise. The only modification to the rotor-stator example is to subtract $\left(c_{p_{f_i}}/2N\right)^2 = \left(0.72/2\right)^2 = 0.11$ from the $\Delta p_f/q_f$ of 0.61. This procedure gives $\Delta p_f/q_f = 0.5$.

It is seen that, for a given flow quantity and rotational speed, the stator-rotor combination gives the highest over-all pressure rise. On the basis of compressibility and maximum-lift limitations, however, the rotor-stator combination will yield the highest pressure rise. (See section "Illustrative Fan Designs.")

It may be remarked that the design criterion for the rotor-stator combination is constant circulation $\gamma\sigma N$ rather than constant static pressure over the blower area because a constant blade circulation will produce a stable rotational-velocity distribution in the downstream flow with no radial velocities. As mentioned in the section "Fan Losses," the rotational velocity does not necessarily represent a loss. Even without guide vanes as such, if the flow is sent through a radiator, much of the rotational energy may be recovered as pressure.

The general design criterion for radial-velocity free downstream flow for the three combinations discussed is, then, constant blade circulation or its equivalent, constant total-pressure increase over the blower plane.

The preceding formulas and the charts for fan design were based on the assumption of initially axial flow. If the initial flow has rotation, as in operation behind a propeller, the fan design is based on the general formulas (8) to (15). For a rotor or stator operating in a flow with initial rotation u_1/V_f, the rotor-stator design charts can still be used to compute c_{p_i} in terms of σc_l and N if the abscissa N of the charts (fig. 6) is replaced by $N + \frac{u_1}{V_f}$. (See equations (8), (10), and (11).) The ideal pressure rise c_{p_i} is regarded as $2\gamma\sigma\left(N + \frac{u_1}{V_f}\right)$. It may be noted also that, for a stator-rotor in a flow with initial rotation u_1/V_f, the stator-rotor charts can be used directly if the design criterion of no downstream rotation

$$\frac{u_1}{V_f} + \gamma_s\sigma_s = \gamma_r\sigma_r$$

is used. The over-all pressure rise without friction is obtained in this case by adding the initial rotational kinetic energy $(u_1/V_f)^2$ to the over-all ideal pressure rise $c_{p_i} = 2\gamma_r\sigma_r N$. Although small amounts of initial rotation will not greatly modify the fan performance, the required blade settings may be appreciably altered.

The calculation of a multistage fan is carried out on a step-by-step basis, each stage being regarded as a single-stage fan operating in an initial flow that is the outgoing flow of the preceding stage. In order to allow for the successive compression of the air by each stage, the fan area may be made successively smaller or the successive stages may be redesigned for smaller rates of flow. The temperature rise across each stage due to adiabatic compression and losses should also be computed as it may lead to excessive operating temperatures in the later stages.

AIRFOIL CHARACTERISTICS FOR CASCADE OPERATION

In the preceding sections, the performance of a fan blade element has been related to the lift and drag coefficients at which the blade is operating. If the isolated airfoil section characteristics (c_l and c_d against α) could be used, the knowledge of the blade-element angle of attack relative to the mean flow velocity would give the blade-element setting to produce the desired performance. This procedure is ordinarily followed in the case of propellers for which the solidity is low. For high-pressure and hence high-solidity fans, the effects of the cascade interference and of the adverse pressure gradient across the fan on the blade section characteristics are no longer negligible.

The problem of predicting cascade-airfoil characteristics for potential flow from a knowledge of the isolated-airfoil characteristics has been attacked in two ways. In the first method, the isolated airfoil is presumed operating at a certain lift and setting relative to the free stream and the necessary changes in airfoil shape and setting to produce the same lift when the airfoil is operating in a cascade are derived. By the second method, the lift of a given airfoil at a given setting in a cascade is determined.

From the first point of view, Betz (reference 5) has given a method based on replacing a thin airfoil by vortices in order to calculate the flow disturbance of the airfoil. As an example of his method, he takes a 5-percent-maximum-camber circular-arc thin airfoil operating at $c_l = 0.7$ and places it in a cascade of solidity $\sigma = 2.03$ and mean flow inclined to the cascade at 45°. In order to maintain the same lift coefficient of 0.7 in cascade operation, the camber must be increased about 30 percent, with relatively small changes in the position of maximum camber and the angle of attack relative to the mean flow.

According to the second method, Collar (references 6 and 7) has solved for the potential flow through cascades of certain airfoil sections including the flat plate. The conclusion is that the relationship from the theory for isolated two-dimensional wings

$$c_l = a_o \sin(\beta - \phi) \tag{34}$$

where β is the blade-element angle, ϕ is the mean-flow angle, and $\beta - \phi = \alpha$ is the angle of attack of the blade element, still holds provided the right-hand side of equation (34) is multiplied

by a factor f and the blade angle β with respect to the mean flow is reckoned from a slightly different angle of zero lift from that of the isolated airfoil. The airfoil shapes given by Collar for which the factor f and the cascade angle of zero lift may be derived theoretically do not resemble very closely the shapes used in practice. A suggested procedure is to use the Collar factor f for flat plates in cascade and the angle of zero lift of the isolated airfoil, corrected for thickness by a method of reference 2. Theoretical curves of the factor f as a function of the solidity $\sigma = \frac{c}{s}$ and blade angle β are given in reference 6 and are reporduced in figures 8 and 9.

The thickness correction (reference 2) is a change δ in the angle of mean air flow relative to the blade element. It is obtained from

$$\tan \delta = \frac{\frac{\pi}{6} D\sigma^2 \sin (\beta + \phi)}{1 - \frac{\pi}{6} D\sigma^2 \cos (\beta + \phi)} \tag{35}$$

where

$$D = \frac{S}{c^2} = \frac{\text{Profile area}}{(\text{Profile chord})^2}$$

is the reciprocal of the blade profile aspect ratio. The correction angle δ has the effect of increasing β of equation (34) to obtain the setting for a given lift coefficient; hence, equation (34) now reads

$$c_l = fa_o \sin (\beta - \phi - \delta) \tag{36}$$

This equation applies to rotors and to stators downstream of rotors if potential flow is assumed. For stators upstream of rotors (turbine action), the sign of the right-hand side of equation (36) is reversed and angles are measured from the blower plane to the convex side of the blade (fig. 10). Note that ϕ is the angle between the mean flow w and the blower plane. The solution of equation (36) for the blade angle β involves several successive approximations because the factor f and the correction δ both depend on β.

Instead of regarding each airfoil of a cascade as operating at a certain lift (and drag) coefficient with respect to the mean relative flow, the cascade as a whole may be viewed as a device for turning the entering flow through a certain angle (references 4 and 8 and unpublished work by Quentin Wald of United Aircraft Corporation). For example, in reference 4, the investigation of a cascade of low-drag airfoils with an initial relative-flow angle of 45° and varying exit flow angles, obtained by varying the blade angle, led the authors to conclude that "the angle through which the air is turned by a cascade of blades with a solidity of 1 and a small camber is nearly equal to the angle of attack (with respect to the entering air) of the blades minus the angle of attack for zero lift of the isolated airfoil."

It may be noted that the turned angle of the flow $\phi_1 - \phi_2$ is expressible in terms of the blade lift coefficient by means of equations (8) and (10), and if drag is neglected,

$$\sigma c_l = \frac{2(\cot \phi_1 - \cot \phi_2)}{\sqrt{1 + \left[N + \frac{u_1}{V_f} - \frac{1}{2}\left(\cot \phi_1 - \cot \phi_2\right)\right]^2}}$$

If the profile drag is large, this expression should be modified by the effect of the tangential component of the drag force in turning the flow.

In addition to the mutual interference previously discussed, which may be termed a velocity interference, the pressure rise (blower action) or drop (turbine action) across the stage affects the boundary-layer phenomena in the stage. For example, the adverse pressure gradient across a fan rotor reduces the lift on the rotor blade, increases the drag, and causes an earlier stall. Experiments on a typical airfoil section (reference 3, figs. 66 and 67) showed that, for a blade angle β of 20° and solidity σ of 0.85, the factor f of equation (36) was unity (although the Collar lift factor f for flat plates was 1.6 in this case), δ was about 1°, and the section stalled at the comparatively low lift coefficient of slightly over 0.7. The value 0.7 has further been approximately substantiated by applying the design method in reverse to some experimentally obtained maximum pressure rises; for example, those of references 4 and 9.

On the basis of the preceding results, which represent typical conditions in a high-speed rotor, the factor f, the angle δ, and the maximum lift coefficient $c_{l_{max}}$ may be assumed to be 1.0, 0.0°, and 0.7, respectively. These values are, of course, provisional and subject to change following more extensive experimental investigation. For this reason, the rotor blade thus designed should be adjusted in operation to give the maximum pressure rise without stalling. If the adjustment is small, the error introduced into the blade twist by this procedure is probably not serious. The interference corrections f and δ should be included in the design of stators for which analyses based on potential flow would be more likely to apply. The maximum lift coefficient of a stator blade likewise should be substantially greater than for a rotor blade.

As to the choice of airfoil, an isolated airfoil section that is efficient at the design point c_l may be chosen (inasmuch as there are no comparative data on airfoils for cascade operation) and warped by the procedure of reference 5 for cascade operation. According to the previously quoted result of reference 5, a 15-percent increase in camber of the isolated airfoil section should suffice for a cascade of solidity $\sigma = 1$. If large flow deflections are to be accomplished, as by a stator, the choice of camber for a stator airfoil section may be guided by the angle through which the flow is to be deflected; that is, the camber may be determined by lining up the tangents at the leading and the trailing edges of the mean line with the initial and the final flow directions, respectively. It is apparent that more experimental results on airfoils in cascade operation are needed to establish the basic data of axial-fan design.

ILLUSTRATIVE FAN DESIGNS

The discussions of the preceding sections will be illustrated by the design of a stator-rotor combination, rotor-stator combination, and rotor operating alone at an altitude of 40,000 feet. The effect of change of altitude will then be considered by estimating the performance of the rotor-stator combination at 20,000 feet.

Each design will be made for maximum pressure rise without stalling the rotor blades and without running into compressibility effects. The first limitation applies to the hub section because the lowest relative velocity, and hence highest lift coefficient for a given pressure rise, occurs there. The second limitation applies to the tip section because it travels at the highest relative speed. These two conditions are expressed as follows: At the hub section, by equations (23) and (31),

$$\left(\sigma_r c_{l_r}\right)_{max} = \frac{c_{p_{f_i}}}{x_h N_o \sqrt{1 + \left(x_h N_o \pm \frac{c_{p_{f_i}}}{4 x_h N_o}\right)^2}} \tag{37}$$

At the tip section, by equations (24) and (32),

$$\left(\frac{w_r}{V_f}\right)_{max} = \sqrt{1 + \left(N_o \pm \frac{c_{p_{f_i}}}{4N_o}\right)^2} \tag{38}$$

where $x_h = \frac{R_h}{R_o}$ and $N_o = \frac{\omega R_o}{V_f}$. The upper sign refers to the stator-rotor combination and the lower to the rotor-stator combination and the rotor alone.

In these equations the values of x_h and V_f are fixed by the rotor dimensions and the desired flow quantity. The maximum value of $\sigma_r c_{l_r}$ is, or should be, known from experiment, as should also w_r from the consideration of compressibility. The two equations can then be solved for N_o and $c_{p_{f_i}}$, which determine the rotational speed and the ideal pressure rise of the fan. The rotation parameter N is then fixed for any other location which, together with the design criterion of constant $c_{p_{f_i}}$, determines the lift coefficient c_{l_r} for any other blade element by using either the design charts (figs. 4 and 6) or equations (23) and (31). The rotor design is completed by estimating the various losses and finally the blade angles to give the required lift coefficients. The stator, if any, is designed from a knowledge of the ideal pressure rise and the condition of complete cancelation of stream rotation. The details are given in the following discussion.

The solution of equations (37) and (38) for $c_{p_{f_i}}$ and N_o is obtained by solving the quadratic

$$au^2 \mp bu - c = 0$$

as

$$u = \frac{\pm b + \sqrt{b^2 + 4ac}}{2a} \tag{39}$$

and then substituting

$$\left.\begin{aligned} N_o &= m \mp u \\ c_{p_{f_i}} &= 4N_o u \end{aligned}\right\} \tag{40}$$

where

$$\left.\begin{aligned} m &= \sqrt{\left[\left(\frac{w_r}{V_f}\right)_{max}\right]^2 - 1} \\ k &= \frac{x_h\left(\sigma_r c_{l_r}\right)_{max}}{4} \\ a &= 1 - k^2\left(\frac{1}{x_h} - x_h\right)^2 \\ b &= 2mk^2\left(1 - x_h{}^2\right) \\ c &= k^2\left(1 + x_h{}^2 m^2\right) \end{aligned}\right\} \tag{41}$$

The upper sign refers to the stator-rotor combination and the lower, to the rotor-stator combination and the rotor alone.

As to the fan dimensions, the outer radius will probably be fixed by considerations of engine or cowling diameter. Assume $R_o = 2$ feet. The inner radius should be such as to keep the solidity at the hub down to a reasonable value and not too different from the solidity at the tip. Also, the resulting fan area should be large compared with the tip-clearance area and should permit efficient diffusing downstream of the fan. Assume an inner radius of 1.55 feet giving a radius ratio $x_h = 0.776$, a fan area $A_f = 5$ square feet, and a blade span of 5.375 inches. If a tip clearance of 1/8 inch or 2.3 percent of the blade span is further assumed, then, according to figure 3, a loss of 8.3 percent of the ideal pressure rise will occur.

The maximum lift coefficient is taken as $c_{l_{max}} = 0.7$ in view of results quoted previously from reference 3. According to some results of reference 2, a rotor with blade chord increasing toward the outer section is more efficient than one with either constant chord or chord decreasing toward the outer section. The reason is connected with the fact that the secondary flows previously mentioned (see section "Theory of the Axial-Flow Fan") cause a dead-air flow toward the blade tips, which may consequently stall first unless the lift coefficient is kept low. A constant-solidity blade with $\sigma_r = 0.85$ is accordingly chosen. The quantity $\sigma_r c_{l_r}$ is therefore $0.7 \times 0.85 = 0.595$.

The maximum relative velocity is determined by the somewhat arbitrary though conservative compressibility criterion that the maximum local relative velocity at the rotor blade is not to exceed 0.9a, where a is the speed of sound at the fan. Inasmuch as the maximum local relative velocity is about 1.31 times the relative velocity and the speed of sound at 40,000 feet is 1000 feet per second, the maximum relative velocity is

$w_{r_{max}} = \frac{0.9}{1.31} \times 1000 = 686$ feet per second. In order to get V_f, the required mass flow is taken as $M = 0.821$ slug per second (see section "Power Losses in a Cooling Installation") which, with a density at the fan of 0.000616 slug per cubic foot and the fan area of 5 square feet, gives $V_f = 266$ feet per second. Therefore, $(w_r/V_f)_{max} = 2.58$.

The values of x_h, $(\sigma_r c_{l_r})_{max}$, and $(w_r/V_f)_{max}$ thus determined are substituted in equations (41), (39), and (40) to give the values of N_o and $c_{p_{f_i}}$ shown in table I. The values of rotational speed derived from N_o are also given. These values of N_o and $c_{p_{f_i}}$ are the basis for the various fan designs given in tables II, III, and IV. The tables contain the itemized design procedure and the necessary references to the text and figures. Some of the results are included for comparison in table I. It appears that the rotor-stator arrangement is capable of producing the greatest pressure rise, though with the requirement of operating at a considerably higher rotational speed. From a consideration of the solution of equations (37) and (38), this result is found to be generally true if

$$m^2 \left(1 - 2x_h^2\right) < 1 + \frac{\left[(\sigma c_l)_{max}\right]^2}{16} \left(1 - x_h^2\right)^2 \left(m^2 - 1\right)$$

Because the second term on the right-hand side is quite small and usually positive, the rotor-stator combination is seen to yield the highest pressure rise if $x_h = R_h/R_o \geqq 0.707$. Below this value the rotor-stator or the stator-rotor combination can yield the higher pressure rise, depending mainly on the value of m.

For operation at an altitude of 20,000 feet, the essential difference is in the air quantity required for cooling. It is assumed that, at 20,000 feet, 1.25 times the mass flow and hence 0.475 times the volume rate of flow at 40,000 feet are necessary. If the rotational speeds were maintained at the original values, the rotor blades would be completely stalled. As can be seen from the performance curves in references 2, 9, and 10, stalling the blades means that the maximum pressure rise is developed but with high losses. If the rotational speeds are diminished in the ratio of 0.475, then N is the same and the nondimensional operation of the fan is the same as at 40,000 feet. Therefore, because

$$\left(\frac{1}{2}\rho V_f^2\right)_{20,000} = 0.6\left(\frac{1}{2}\rho V_f^2\right)_{40,000}$$

the actual pressure rises of any of the combinations will be about 0.6 of the values at 40,000 feet. With fixed blades this performance is about all that can be achieved at the lower altitude on the assumption that $c_{l_{r_{max}}} = 0.7$. If the rotor and stator blade angles are adjustable, however, and the rotor speed is maintained at 3310 rpm for the rotor-stator arrangement, then for a hub-section value of $\sigma_r c_{l_r} = 0.595$ and $N_h = \frac{2.022}{0.475} = 4.26$, figure 6(b) gives a $(\Delta p_f/q_f)_{ideal}$ of 9.8. If the same efficiency as at 40,000 feet is assumed, the actual $\Delta p_f/q_f$ is $0.9 \times 9.8 = 8.8$ and Δp_f is 22 inches of water, as compared with 9.1 inches at 40,000 feet. The twist of the blade is incorrect at the lower altitude, however. In this case it is desired to calculate the pressure rise at any radial location from a knowledge of the blade angle and N for the location. The solidity σ and interference corrections f and δ, if any, are also known. The ideal pressure rise is given directly in terms of these quantities by eliminating c_{l_r} from

$$\sigma_r c_{l_r} = \frac{c_{p_{f_i}}}{N\sqrt{1 + \left(N \pm \frac{c_{p_{f_i}}}{4N}\right)^2}}$$

and, by equation (36),

$$c_{l_r} = fa_o \sin (\beta - \phi_r - \delta)$$

where

$$\frac{1}{\sin \phi_r} = \sqrt{1 + \left(N \pm \frac{c_{p_{f_i}}}{4N}\right)^2}$$

The result is

$$c_{p_{f_i}} = \frac{\sigma_r f a_o N[N \sin (\beta - \delta) - \cos (\beta - \delta)]}{1 \pm \frac{\sigma_r f a_o}{4} \sin (\beta - \delta)} \tag{42}$$

where the minus sign refers to the stator-rotor combination and the plus sign refers to the rotor-stator combination, which includes also the case of rotor alone. (See section "Rotor Alone.") It is assumed in equation (42) that, if a stator is used, it is kept adjusted in such a way that no stream rotation exists downstream of the blower. The error caused by using equation (42) with fixed stator is small for a rotor-stator but not for a stator-rotor combination. In the stator-rotor arrangement, the stator and rotor should be analyzed separately by means of the general formulas (8), (10), (11), and (36). The actual pressure rise is obtained from equation (10) applied to rotor and stator. This pressure rise will not actually be obtained if the rotor maximum section lift coefficient is exceeded. Furthermore, if the pressure rises vary greatly over the blower area, they should be averaged by the method of reference 2.

The design method presented in the preceding sections has been used to compute the known performance of existing fans such as that of reference 9. The results of these and of other computations for new designs, which have subsequently been tested, show that the method predicts performance satisfactorily, although an experimental adjustment of the blade setting may be necessary. (See section "Airfoil Characteristics for Cascade Operation.")

POWER LOSSES IN A COOLING INSTALLATION

It is appropriate to conclude with a discussion of the internal-cooling-power losses in a cooling installation that includes a fan. The statement in the "Introduction" that the power required to drive a fan may be more than recovered by means of the higher exit velocity of the cooling air thus attainable will incidentally be justified.

The internal cooling power is the sum of the power input to the fan and the momentum power of the cooling air. The power input to the fan per unit mass flow of cooling air is a function of the fan pressure rise and the state of the air in front of the fan. The momentum power per unit mass is the product of the free-stream velocity and the difference between free-stream and ultimate wake velocity of the cooling air. External cooling power, such as caused by excessive flap deflections with resulting increase of drag, is not discussed herein. This component of the total cooling power can be included in an analysis of an actual cooling installation by means of experimental cowl-flap data. Likewise, drag increments due to the weight of the component parts are not considered.

A cooling installation of cowling, fan, cooling resistance (such as engine or radiator), and exit is represented schematically in figure 11(a). Cooling air, regarded as compressible, enters and undergoes adiabatic but not isentropic compression from state 0 to state f1. The total energy per unit mass of air remains constant in this process, that is,

$$c_p T_o + \frac{V_o^2}{2} = c_p T_{f1} + \frac{V_{f1}^2}{2}$$

but the inlet duct causes a stagnation pressure drop Δp_i. By a stagnation pressure drop across a resistance is meant a pressure drop measured between, or corrected to, two stagnation regions before and behind the resistance. Next, the fan increases the total energy per unit mass by

$$\frac{P_f}{M} = c_p(T_{f2} - T_{f1}) + \frac{1}{2}(V_{f2}^2 - V_{f1}^2) \qquad (43)$$

while the pressure rises from p_{f1} to p_{f2}. The air then passes through the fan diffuser in which a stagnation pressure drop Δp_d occurs at constant total energy. At state 1, which is the near-stagnation condition just in front of the cooling resistance, a fraction of the engine-heat rejection may be added to the part of

the flow that goes through the resistance proper. This flow then expands isentropically into the resistance area, state 2. From state 2 to the resistance exit, state 3e, the cooling air is increased in total energy by the remainder of the heat rejection and suffers most of the cooling pressure drop. At state 3e the flow is ejected into the large space at state 3, the pressure and total energy remaining constant, with the result that the kinetic energy of the air at state 3e is largely lost. The cooling-resistance pressure drop is thus $\Delta p_r = p_3 - p_1$. The entire flow at state 3 then expands almost isentropically, with constant total energy, from its practically stagnation condition at state 3 to the ultimate exit conditions p_o and V_4.

The power input to the fan is given by equation (43). The second term on the right is negligible for a single-stage fan with constant flow area, whereas in a multistage fan the flow area is adjusted to keep a constant axial velocity. The first term can be written in terms of the initial state and pressure ratio across the fan by using the isentropic compression formula $T \propto p^{\frac{\gamma-1}{\gamma}}$. The power input to the fan thus becomes

$$P_f = Mc_p(T_{f2} - T_{f1})$$

$$= \frac{\gamma M P_1}{(\gamma-1)\eta_f \rho_1}\left[\left(1 + \frac{\Delta p_f}{p_1}\right)^{\frac{\gamma-1}{\gamma}} - 1\right]$$

$$= \frac{M\Delta p_f}{\eta_f \rho_1}\left[1 - \frac{1}{2\gamma}\frac{\Delta p_f}{p_1} + \ldots\right] \qquad (44)$$

The fan efficiency η_f in this expression takes account of the fact that the compression is not quite isentropic and that consequently the actual final temperature T_{f2} is greater than the isentropic final temperature would be for the same pressure rise.

The momentum power of the installation is, by the momentum equation,

$$P_m = MV_o(V_o - V_4) \qquad (45)$$

The ultimate exit velocity V_4, at which the pressure is that of the free stream p_o, is determined by the condition of constant total energy from states 3 to 4:

$$c_p T_3 = c_p T_4 + \frac{V_4^2}{2}$$

$$\frac{V_4^2}{2} = c_p T_3 \left(1 - \frac{T_4}{T_3}\right) \tag{46}$$

The quantity $1 - \frac{T_4}{T_3}$ is the Meredith effect efficiency, that is, the efficiency of conversion of energy at state 3 to kinetic energy of the wake at state 4. For isentropic expansion between states 3 and 4, it may be expressed as

$$1 - \frac{T_4}{T_3} = 1 - \left(\frac{p_o}{p_3}\right)^{\frac{\gamma-1}{\gamma}} \tag{47}$$

If conditions between states 3 and 4 differ considerably from the isentropic, equation (47) must be modified. For well-designed outlet ducts, no modification of equation (47) is necessary. The pressure at state 3 is the free-stream stagnation pressure p_s plus the sum of the stagnation-pressure changes up to state 3

$$p_3 = p_s + \Delta p_f - \Delta p_i - \Delta p_d - \Delta p_r \tag{48}$$

The total energy per unit mass at state 3 is the free-stream total energy plus the total-energy additions in the installation:

$$c_p T_3 = c_p T_o + \frac{V_o^2}{2} + \frac{P_f}{M} + \frac{H}{M} \tag{49}$$

The substitution of equations (49), (48), and (47) in equation (46) yields for the exit velocity

$$\frac{V_4^2}{2} = \left(c_p T_o + \frac{V_o^2}{2} + \frac{P_f}{M} + \frac{H}{M}\right)\left[1 - \left(\frac{p_o}{p_s + \Delta p_f - \Delta p_i - \Delta p_d - \Delta p_r}\right)^{\frac{\gamma-1}{\gamma}}\right] \tag{50}$$

which determines the momentum power by equation (45). The sum of equations (44) and (45) is then the internal-cooling-power loss of the installation.

Before equation (50) can be used, the cooling and fan-diffuser stagnation-pressure drops Δp_r and Δp_d as well as the required mass flow M must be determined as a function of the fan pressure rise Δp_f. This procedure is necessary because the fan ahead of the cooling resistance increases the temperature and density ahead of the cooler, thereby increasing the required mass flow for cooling but decreasing (not always) the cooling pressure drop. The determination is made by a step-by-step process similar to the processes of references 11 and 12.

In order to get M, Δp_r, and Δp_d as functions of Δp_f, the pressure and temperature just ahead of the cooler are needed. The following equations determine the pressure and the temperature in front of the cooler, as well as the mass flow, as functions of fan pressure rise:

(a) Free stream to state f1, constant total energy:

$$c_p T_o + \frac{1}{2} V_o^2 = c_p T_{f1} + \frac{1}{2} V_{f1}^2$$

(b) Pressure and density at state f1, inlet diffusing efficiency η_i:

$$p_{f1} = p_o \left(\frac{T_{f1}}{T_o} \right)^{\frac{\gamma}{\gamma-1}} - (1 - \eta_i) q_o$$

$$\rho_{f1} = p_{f1} / R T_{f1}$$

(c) Pressure and temperature rise across fan, fan efficiency η_f:

$$\frac{p_{f2}}{p_{f1}} = \left[\eta_f \frac{T_{f2}}{T_{f1}} + (1 - \eta_f) \right]^{\frac{\gamma}{\gamma-1}}$$

(d) Pressure and density at state f2:

$$p_{f2} = p_{f1} \left(\frac{p_{f2}}{p_{f1}} \right)$$

$$\Delta p_f = p_{f2} - p_{f1} \qquad \rho_{f2} = p_{f2} / R T_{f2}$$

(e) State f2 to state 1, constant total energy:

$$c_p T_1' = c_p T_{f2} + \frac{1}{2} V_f^2$$

(f) Pressure at state 1, fan-diffuser efficiency η_d:

$$p_1 = p_{f2} \left(\frac{T_1'}{T_{f2}} \right)^{\frac{\gamma}{\gamma-1}} - (1 - \eta_d) q_{f2}$$

where

$$q_{f2} = \frac{1}{2} \rho_{f2} V_{f2}^2$$

(g) Variation of mass flow M with cooler entrance temperature T_1', where T_1' is the temperature in state 1, before any of the heat is added to it. This variation is determined by a cooling correlation for the cooler. (See references 11 and 12.) Figure 12 illustrates this variation for the air-cooled engine of the illustrative example given hereinafter.

(h) Equation of continuity at fan

$$M = \rho_{f2} V_f A_{f2} \qquad M = \rho_{f1} V_f A_{f1}$$

(51)

In these equations the atmospheric conditions p_o, T_o, flight speed V_o, and efficiencies η_i, η_f, η_d are all known. Furthermore, either the fan entrance area A_{f1} is given and the fan exit area A_{f2} regarded as variable to maintain constant axial velocity V_f, or vice versa. In the following illustrative example, the value of A_{f1} was assumed, although about the same results would be obtained in either case. With an assumed V_f, the following quantities are determined in order from equation (51): T_{f1} from (a); p_{f1} and ρ_{f1} from (b); M from (h); T_1' from (g); T_{f2} from (e); p_{f2}/p_{f1} from (c); p_{f2}, Δp_f, ρ_{f2} from (d); q_{f2} and p_1 from (f). The temperature T_1' is then increased to T_1 by the heat rejection, if any, ahead of the cooler. In addition, the value of $G = \rho_2 V_2$ is determined as a certain fraction of M. The proportionality between G and M can be obtained from the sea-level data for the cooler by performing the cooler pressure-drop calculation in reverse to find G corresponding to the known pressure drop.

From the values of p_1, T_1, and G corresponding to a fan pressure rise Δp_f, the pressure drop Δp_r across the cooler can be determined in two steps. First, if only the air that goes through the cooler proper (in an air-cooled engine this amount is less than the total mass flow) is considered, the state of the air at station 2 is determined by Bernoulli's equation, which may be written

$$\frac{\left(\frac{p_1}{p_2}\right)^{\frac{\gamma-1}{\gamma}} - 1}{\left(\frac{p_1}{p_2}\right)^{\frac{\gamma+1}{\gamma}}} = \frac{R^2 G^2 T_1}{2 c_p p_1^2} \equiv K \tag{52}$$

This equation can be solved for p_1/p_2 with the aid of figure 13, which gives p_1/p_2 against K for $\gamma = 1.4$, $R = 1715$, and $c_p = 6020$ in foot-pound-second units. The temperature at station 2 is given by

$$\frac{T_1}{T_2} = \left(\frac{p_1}{p_2}\right)^{\frac{\gamma-1}{\gamma}}$$

Secondly, the pressure at the baffle exit, station 3e, is determined by an equation based on heat-transfer and skin-friction considerations. (See references 11 and 12.)

$$\log_e \frac{p_2}{p_3} \frac{T_w - T_2}{T_w - T_{3e}} \frac{T_{3e}}{T_2} = \frac{p_2^2}{RG^2(T_2 + T_{3e})} \left[1 - \left(\frac{p_3}{p_2} \right)^2 \right] \qquad (53)$$

in which T_{3e} is greater than T_2 by an amount corresponding to the heat added from stations 2 to 3e and T_w is the estimated average engine temperature. Equation (53) is plotted in figure 14 for a range of the parameters $\frac{T_w - T_2}{T_w - T_{3e}} \frac{T_{3e}}{T_2}$ and $\frac{p_2^2}{RG^2(T_2 + T_{3e})}$.

The total energy c_pT_3 behind the cooler is calculated by equation (49), using the first one of equations (44) for the P_f/M term. The values of c_pT_3 and p_3 can now be substituted directly in equation (46) to give the exit velocity V_4 and the calculation is completed by equations (44) and (45).

For the fan behind the resistance and for the station numbering as in figure 11(b), the expression through equation (50) previously derived hold without change. The calculations are greatly simplified in this case because M and Δp_r are constant at the values given by the preceding method for $\Delta p_f = 0$. Conditions at the fan can be conveniently determined from the stagnation conditions behind the cooler and the mass flow by using figure 13.

The calculations previously outlined for the fan ahead of the cooling resistance were carried through for an air-cooled engine. The following data, based on an actual proposed cooling installation, were assumed:

Altitude (Army air), feet	40,000
Atmospheric pressure, p_o, pounds per square foot	391.9
Atmospheric density, ρ_o, slug per cubic foot	0.000550
Atmospheric temperature, T_o, °F absolute	415.4
Specific heat at constant pressure, c_p, foot-pounds per slug per °F absolute	6020
Ratio of specific heats, γ	1.40
Inlet-duct efficiency, η_i	0.90
Fan efficiency, η_f	0.80
Fan-diffuser efficiency, η_d	0.90
Fan-entrance area, A_{f1}, square feet	5
Engine heat rejection, H, foot-pounds per second	550,000
Flight speed, V_o, feet per second	587

In addition the following assumptions were made: Figure 12 for M against T_1'; $G = 0.305M$; one-half the heat rejection added ahead of the baffles and one-half in the baffles; 80 percent of the total mass flow through the baffles; the average engine temperature $T_w = 888^\circ$ F absolute.

The results are given in figures 15 and 16. Some of the various cooling-air quantities are shown in figure 15. The variation with fan pressure rise is practically linear in all cases, a fact that may be used to reduce the labor of subsequent calculation. The engine pressure drop $p_3 - p_1$ decreased from 26 inches of water at $\Delta p_f = 0$ to 24 inches of water at $\Delta p_f = 38$ inches of water. For high-enough fan compression, the temperature of compression tends to compensate for the effect of the increased density in reducing the engine pressure drop.

The variation of fan and momentum power and of their sum, the internal cooling power, is shown in figure 16. The internal cooling power is large, varying from a maximum of 640 horsepower to a minimum of 330 horsepower. It is seen that, without a fan, there is a cooling-pressure deficiency of 8 inches of water. The cowl-flap deflection required to overcome this deficiency (about $0.5q_0$) would result in a cooling-power loss much greater than the indicated maximum value of 640 horsepower. A fan is therefore essential. The maximum estimated pressure rise from a single-stage fan is indicated in figure 16 as 8.5 inches of water. This value was obtained by multiplying the value of 9.1 inches in table I by 80/85.6 to make the fan efficiency consistent with that assumed in this example. This pressure rise reduces the internal cooling power to 520 horsepower. Two stages would decrease this value to 350 horsepower, which is only 20 horsepower above the minimum possible cooling-power loss. In order to reduce the minimum cooling-power loss, the required engine pressure drop for the given heat rejection would have to be reduced, for example, by improving the finning. The flight speed chosen for the calculations was 400 miles per hour. If the speed is reduced, as in climbing, the cooling-pressure deficiency increases. For example, at 310 miles per hour, the deficiency would be about twice the value at 400 miles per hour. A two-stage fan would therefore be necessary to enable climbing without opening the flaps.

It is of interest to note that, at the point of minimum total internal power, the fan power is increasing at the same rate as the thrust (negative momentum) power; hence, the efficiency of conversion of additional power input to the fan into thrust power

is 100 percent at this point. This efficiency drops off for larger additional power inputs to the fan. The possible saving of power, as compared with putting this power into the external propeller, however, is small.

The question of the advisability of locating the fan behind the engine, or cooling resistance, can be answered in the negative, at least for conditions approximating those of the example. Some comparative calculations of fan before and behind the engine showed that the cooling power was of the order of twice as much as with the fan in front. Furthermore, the maximum performance of a single-stage fan was only about 60 percent of that with the fan in front. The main reason for this behavior was that the density behind the engine was about half that in front. Consequently, the volume rate of flow for a given mass flow was double and the power input to the fan for a given pressure rise, roughly $Q\Delta p$, about double. A contributing factor is the increased engine pressure drop, which shifts the momentum-power curve to the right and consequently increases the total internal power. The decreased maximum performance of a single stage is a consequence of the lower density in combination with the higher ratio of axial-flow velocity to fan rotational speed.

The method of internal-power calculation given is an accurate one. The results are sensitive, however, to the values of the various pressure drops, particularly to the pressure drop of the cooling resistance. It is important, therefore, to be reasonably sure of the data that determine the engine pressure drop before indulging in a detailed internal-power analysis. It may be mentioned here that the method of calculating the exit velocity by Bernoulli's equation for incompressible flow, that is,

$$\sum_{i,f,d,r} \Delta p = \frac{1}{2}\rho\left(V_4^2 - V_o^2\right)$$

can lead to large errors on the pessimistic side, particularly for large pressure and density changes through the system.

It is evident that the choice of an axial-flow fan for high-altitude cooling depends on considerations of internal cooling power as well as on marginal cooling-pressure deficiency, structural, and mechanical considerations. In the illustrative example, a two-stage rotor-stator fan arrangement ahead of the engine would be recommended. If the rotational speed could not be achieved because of mechanical difficulties, a stator-rotor arrangement

could be used although at the probable sacrifice of some performance. (See table I.) The stator-rotor arrangement might also be advantageous if the flow conditions ahead of the fan were not uniform, with the result that the guiding and stabilizing effect of a set of stator vanes was needed. Some type of rotational-speed adjustment is also desirable, particularly on high-speed fans, in order to avoid blade stalling at the lower altitudes where smaller volumes of air are required.

CONCLUSIONS

The following conclusions are indicated by the results of the present study of the theory, design, and effect on cooling of the constant-velocity axial-flow fan as related to the problem of high-altitude aircraft engine cooling:

1. An axial-flow fan may be used to give a moderate pressure rise to a large flow quantity of air. Typical performance of a 4-foot-diameter single-stage rotor-stator fan at 40,000-foot altitude is 9 inches of water pressure rise at a flow quantity of 80,000 cubic feet per minute and a rotational speed of 3300 rpm.

2. Existing theory provides a satisfactory basis for the design of axial-flow fans.

3. The use of stationary guide vanes and small rotor tip clearances is essential for efficient fan design.

4. Further research is needed for the development of airfoil sections especially suitable for use in high-speed, high-solidity rotors.

5. The losses in internal cooling power at high altitude are large when the cooling is marginal.

6. An axial-flow fan more than pays for itself in cooling power saved when cooling conditions are marginal.

Langley Memorial Aeronautical Laboratory
National Advisory Committee for Aeronautics
Langley Field, Va.

REFERENCES

1. Silverstein, Abe: High-Altitude Cooling. I - Résumé of the Cooling Problem. NACA ARR No. L4I11, 1944.

2. Ruden, P.: Investigation of Single Stage Axial Fans. NACA TM No. 1062, 1944.

3. Keller, Curt, and Marks, Lionel S.: The Theory and Performance of Axial-Flow Fans. McGraw-Hill Book Co., Inc., 1937.

4. Kantrowitz, Arthur, and Daum, Fred L.: Preliminary Experimental Investigation of Airfoils in Cascade. NACA CB, July 1942.

5. Betz, Albert: Diagrams for Calculation of Airfoil Lattices. NACA TM No. 1022, 1942.

6. Collar, A. R.: Cascade Theory and the Design of Fan Straighteners. R. & M. No. 1885, British A.R.C., 1940.

7. Collar, A. R.: The Flow of a Perfect Fluid through Cascades of Airfoils. Jour. R.A.S., vol. XLV, no. 365, May 1941, pp. 183-213.

8. Wattendorf, Frank L.: The Ideal Performance of Curved-Lattice Fans. Theodore von Kármán Anniversary Volume, Calif. Inst. Technology (Pasadena), 1941, pp. 285-292.

9. Bell, E. Barton: Test of a Single-Stage Axial-Flow Fan. NACA Rep. No. 729, 1942.

10. Struve, E.: Theoretical Determination of Axial Fan Performance. NACA TM No. 1042, 1943.

11. Williams, David T.: High-Altitude Cooling. II - Air-Cooled Engines. NACA ARR No. L4I11a, 1944.

12. Nielsen, Jack N.: High-Altitude Cooling. III - Radiators. NACA ARR No. L4I11b, 1944.

TABLE I - FAN PERFORMANCE BASED ON MAXIMUM-LIFT AND COMPRESSIBILITY CRITERIONS

Fan arrangement	$N_o = \frac{\omega R_o}{V_f}$	$c_{p_{f_i}} = \left(\frac{\Delta p_f}{q_f}\right)_i$	Rotational speed (rpm)	Pressure rise (in. of water)	Input (hp)	Efficiency (percent)
Stator-rotor	2.12	2.17	2700	8.1	120	85.5
Rotor-stator	2.61	2.40	3310	9.1	133	85.6
Rotor alone	2.61	2.40	3310	7.9	133	75.1

National Advisory Committee
for Aeronautics

TABLE II - ILLUSTRATIVE FAN DESIGN - STATOR-ROTOR COMBINATION
[NACA 6512 blade section]

Fan quantity	Source	Calculated values		
Rotor, 32 blades				
$x = \frac{r}{R_o}$		0.776	0.888	1
r, ft		1.552	1.776	2
$N = \frac{\omega r}{V_f}$		1.649	1.885	2.122
$\sigma_r c_{l_r}$	Fig. 4	0.595	0.481	0.396
σ_r		0.85	0.85	0.85
Chord, c_r, in. from σ_r and 32 blades		3.11	3.56	4.01
c_{l_r} for constant $c_{p_{f_i}}$	Fig. 4 or equation (23)	0.7	0.566	0.466
w_r/V_f	Fig. 5	2.22	2.391	2.58
$\left(\frac{\Delta p_f}{q_f}\right)_i = c_{p_{f_i}}$	Equation (40)	2.170	2.170	2.170
$\left(\frac{\Delta p_f}{q_f}\right)_{d_s} = \sigma_s c_{d_s} \frac{w_s}{V_f}$ (c_{d_s} = 0.013, assumed)	See stator data	0.0174	0.0151	0.0133
$\left(\frac{\Delta p_f}{q_f}\right)_{d_r} = \sigma_r c_{d_r} \frac{w_r}{V_f}$ (c_{d_r} = 0.013, assumed)	Equation (19)	0.0245	0.0264	0.0285
$\left(\frac{\Delta p_f}{q_f}\right)_t$ for 2.78-percent clearance	Fig. 3	0.180	0.180	0.180

National Advisory Committee
for Aeronautics

TABLE II - ILLUSTRATIVE FAN DESIGN - Continued.

Fan quantity	Source	Calculated values		
Rotor, 32 blades				
$\left(\frac{\Delta p_f}{q_f}\right)_{resultant} = \left(\frac{\Delta p_f}{q_f}\right)_i - \left[\left(\frac{\Delta p_f}{q_f}\right)_{d_s} + \left(\frac{\Delta p_f}{q_f}\right)_{d_r} + \left(\frac{\Delta p_f}{q_f}\right)_t\right]$		1.948	1.948	1.948
Δp_f, in. water		8.14	8.14	8.14
c_T	Equation (12)	1.365	1.207	1.090
Section efficiency, percent, $\eta = \frac{\left(\frac{\Delta p_f}{q_f}\right)_{resultant}}{Nc_T}$	Equation (15)	86.6	85.6	84.2
Output, $Q\Delta p_f$, hp		102.5		
Input = $\frac{\text{Output}}{\text{Av. efficiency}}$, hp		120		
Mean flow, deg, $\phi = \sin^{-1}\frac{1}{w_r/V_f}$	Fig. 5	26.77	24.71	22.82
$\beta - \phi$ with no interference corrections f and δ and $a_o = 5.65$	Equation (34)	7.11	5.74	4.74
β measured from zero-lift line		33.88	30.45	27.56
β' measured from chord line for $\alpha_{l_o} = 6.2^\circ$		27.68	24.25	21.36

National Advisory Committee
for Aeronautics

TABLE II - ILLUSTRATIVE FAN DESIGN - Concluded.

Fan quantity	Source	Calculated values		
Stator, 39 blades				
$x = r/R_o$		0.776	0.888	1
$\frac{\gamma\sigma}{2} = \frac{(\Delta p_f/q_f)_i}{4N}$	Equation (25)	0.329	0.288	0.2555
σ_s assumed to give reasonable c_{l_s}		1.275	1.116	0.990
Chord, c_s, in. from σ_s and 39 blades		3.83	3.83	3.83
γ_s		0.516	0.516	0.516
$\frac{w_s}{V_f} = \sqrt{1 + \left(\frac{\gamma\sigma}{2}\right)^2}$	Equation (16)	1.051	1.0405	1.031
$c_{l_s} = \frac{2\gamma_s}{w_s/V_f}$	Equation (8)	0.981	0.991	1
$\left(\frac{\Delta p_f}{q_f}\right)_{d_s} = \sigma_s c_{d_s} \frac{w_s}{V_f}$	Equation (17)	0.0174	0.0151	0.0133
$\phi = \sin^{-1} \frac{1}{w_s/V_f}$, deg		72.0	73.75	75.70
$\frac{\pi}{6} D\sigma^2$ for $D = 0.08$		0.0682	0.0524	0.0411
f	for $a_o = 5.65$	0.58	0.62	0.66
δ		2.88	2.11	1.55
$\phi + \delta - \beta$		17.41	16.44	15.55
β		57.47	59.42	61.70
β' for $\alpha_{l_o} = 6.2^\circ$		63.67	65.62	67.90

National Advisory Committee
for Aeronautics

TABLE III - ILLUSTRATIVE FAN DESIGN - ROTOR-STATOR COMBINATION

[NACA 6512 blade section]

Fan quantity	Source	Calculated values		
Rotor, 32 blades				
$x = \frac{r}{R_o}$		0.776	0.888	1
r, ft		1.552	1.776	2
$N = \frac{\omega r}{V_f}$		2.022	2.316	2.609
$\sigma_r c_{l_r}$	Fig. 6	0.595	0.455	0.358
σ_r		0.85	0.85	0.85
Chord, c_r, in. from σ_r and 32 blades		3.11	3.56	4.01
c_{l_r} for constant $c_{p_{f_i}}$	Fig. 6 or equation (31)	0.7	0.536	0.421
w_r/V_f	Fig. 7	1.994	2.287	2.58
$\left(\frac{\Delta p_f}{q_f}\right)_i = c_{p_{f_i}}$	Equation (40)	2.404	2.404	2.404
$\left(\frac{\Delta p_f}{q_f}\right)_{d_s} = \sigma_s c_{d_s} \frac{w_s}{V_f}$ ($c_{d_s} = 0.013$, assumed)	See stator data	0.0157	0.0136	0.0120
$\left(\frac{\Delta p_f}{q_f}\right)_{d_r} = \sigma_r c_{d_r} \frac{w_r}{V_f}$ ($c_{d_r} = 0.013$, assumed)	Equation (27)	0.0220	0.0253	0.0285

National Advisory Committee for Aeronautics

TABLE III - ILLUSTRATIVE FAN DESIGN - Continued.

Fan quantity	Source	Calculated values		
Rotor, 32 blades				
$\left(\frac{\Delta p_f}{q_f}\right)_t$ for 2.78-percent clearance	Fig. 3	0.200	0.200	0.200
$\left(\frac{\Delta p_f}{q_f}\right)_{resultant}$		2.166	2.166	2.163
Δp_f, in. water		9.06	9.06	9.05
c_T	Equation (28)	1.227	1.090	0.990
Section efficiency, percent, $\eta = \frac{\left(\frac{\Delta p_f}{q_f}\right)_{resultant}}{Nc_T}$	Equation (15)	87.2	85.8	83.8
Output, $Q\Delta p_f$, hp		115		
Input = Output/Av. efficiency, hp		133		
$\phi = \sin^{-1}\frac{1}{w_r/V_f}$, deg	Fig. 7	30.13	25.94	22.81
$\beta - \phi$ for $a_o = 5.65$	Equation (34)	7.11	5.44	4.28
β		37.24	31.38	27.09
β' for $\alpha_{l_o} = 6.2^\circ$		31.04	25.18	20.89

National Advisory Committee
for Aeronautics

TABLE III - ILLUSTRATIVE FAN DESIGN - Concluded.

Fan quantity	Source	Calculated values		
Stator, 39 blades				
x		0.776	0.888	1
$\frac{\gamma\sigma}{2} = \frac{(\Delta p_f/q_f)_i}{4N}$	From rotor calculations	0.297	0.260	0.231
σ_s (assumed)		1.159	1.015	0.901
Chord, c_s, in. from σ_s and 39 blades		3.49	3.49	3.49
γ_s		0.513	0.513	0.513
$\frac{w_s}{V_f} = \sqrt{1 + \left(\frac{\gamma\sigma}{2}\right)^2}$		1.041	1.032	1.026
$c_{l_s} = \frac{2\gamma_s}{w_s/V_f}$	Equation (8)	0.986	0.995	1
$\left(\frac{\Delta p_f}{q_f}\right)_{d_s} = \sigma_s c_{d_s} \frac{w_s}{V_f}$	Equation (29)	0.0157	0.0136	0.0120
$\phi = \sin^{-1} \frac{1}{w_s/V_f}$		73.69	75.51	76.90
$\frac{\pi}{6} D\sigma^2$	Fig. 8 and equations (35) and (36)	0.0562	0.0432	0.0340
f		0.525	0.58	0.63
δ		0.67	0.45	0.31
$\beta-\phi-\delta$		19.42	17.68	16.31
for $D = 0.08$				
β		93.78	93.64	93.52
β' for $\alpha_{l_o} = -6.2^\circ$		87.58	87.44	87.32

National Advisory Committee
for Aeronautics

TABLE IV - ILLUSTRATIVE FAN DESIGN - ROTOR ALONE

[NACA 6512 blade section; 32 blades]

Fan quantity	Source	Calculated values		
x	(a)	(a)	(a)	(a)
r				
N				
$\sigma_r c_{l_r}$				
σ_r				
c_r				
c_{l_r}				
w_r/V_f				
$\left(\frac{\Delta p_f}{q_f}\right)_i = c_{p_{f_i}}$ for rotor-stator		2.404	2.404	2.404
$\left(\frac{\Delta p_f}{q_f}\right)_{\text{rotational energy}} = (\gamma\sigma)^2 = \left[\frac{(\Delta p_f/q_f)_i}{2N}\right]^2$	Equation (33)	0.353	0.270	0.212

[a]Same as in table III.

National Advisory Committee
for Aeronautics

TABLE IV - ILLUSTRATIVE FAN DESIGN - Concluded.

Fan quantity	Source	Calculated values		
$\left(\frac{\Delta p_f}{q_f}\right)_{d_r}$	(b)	0.022	0.025	0.029
$\left(\frac{\Delta p_f}{q_f}\right)_t$	(b)	0.200	0.200	0.200
$\left(\frac{\Delta p_f}{q_f}\right)_{resultant}$	(b)	1.829	1.909	1.963
Δp_f, in. water	(b)	7.64	7.98	8.20
c_T	(b)	1.227	1.090	0.990
Section efficiency, η	(b)	73.6	75.6	76.0
Output, $Q(\Delta p_f)_{av}$ hp		100		
Input = $\frac{\text{Output}}{\text{Av. efficiency}}$, hp		133		
ϕ	(a)	(a)	(a)	(a)
$\beta-\phi$	(a)			
β	(a)			
β'	(a)			

[a]Same as in table III.

[b]Formulas and references same as in table III.

National Advisory Committee
for Aeronautics

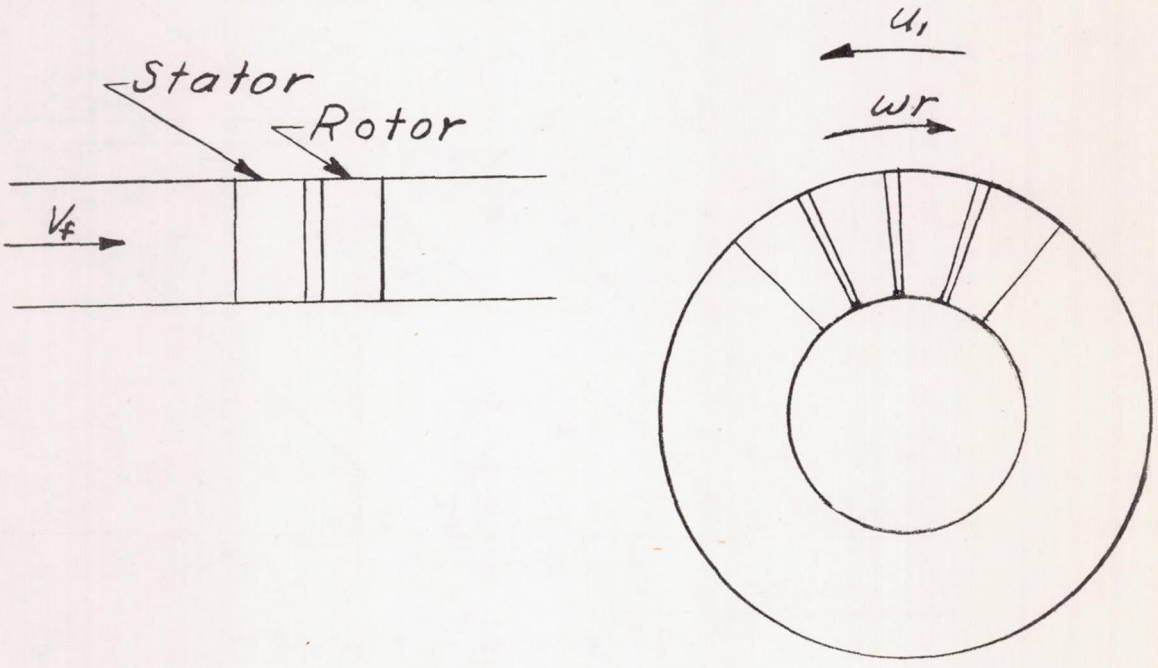

Figure 1.- Typical axial-flow-fan stage.

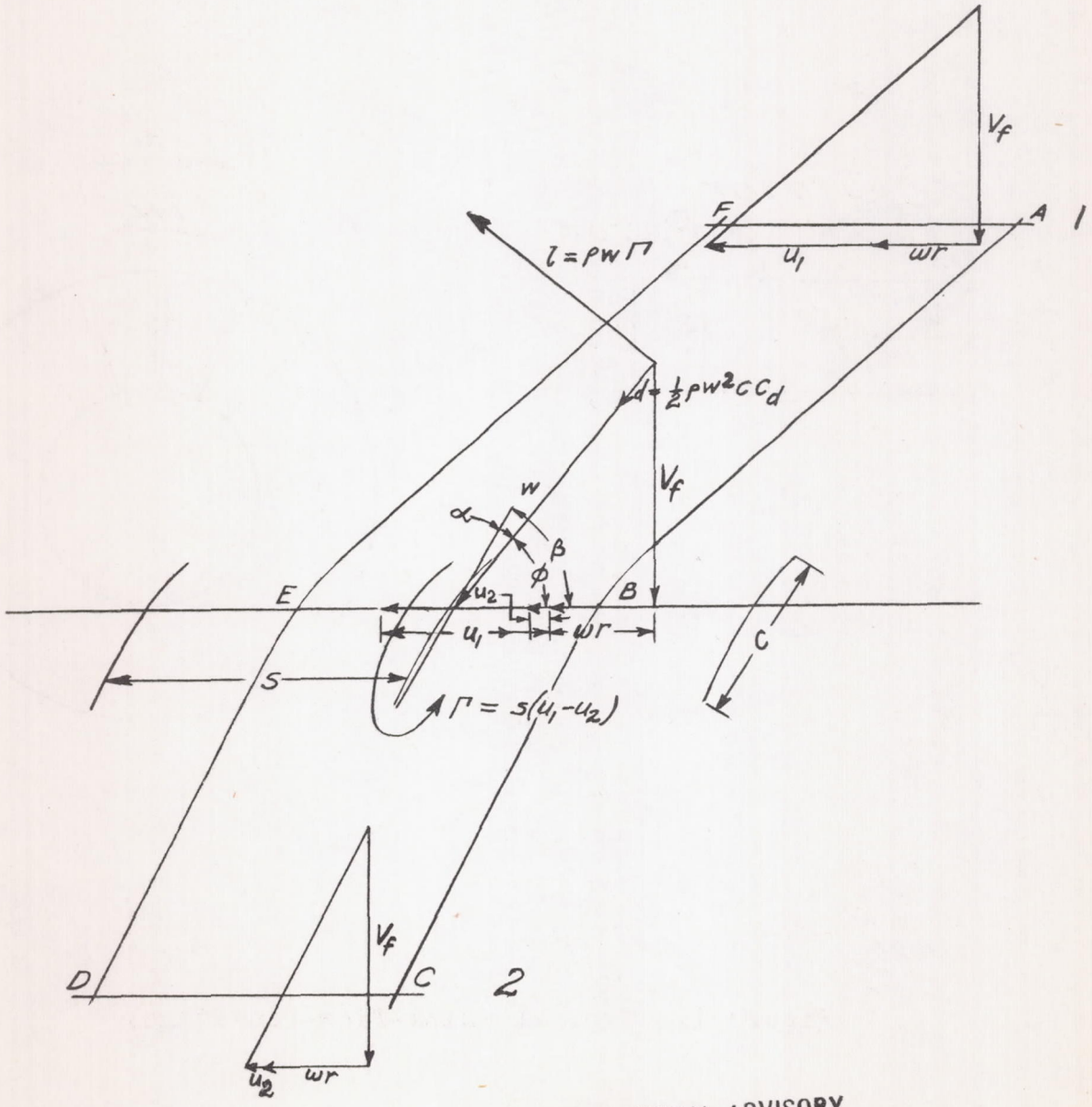

NATIONAL ADVISORY
COMMITTEE FOR AERONAUTICS

Figure 2. - Rotor forces and velocities.

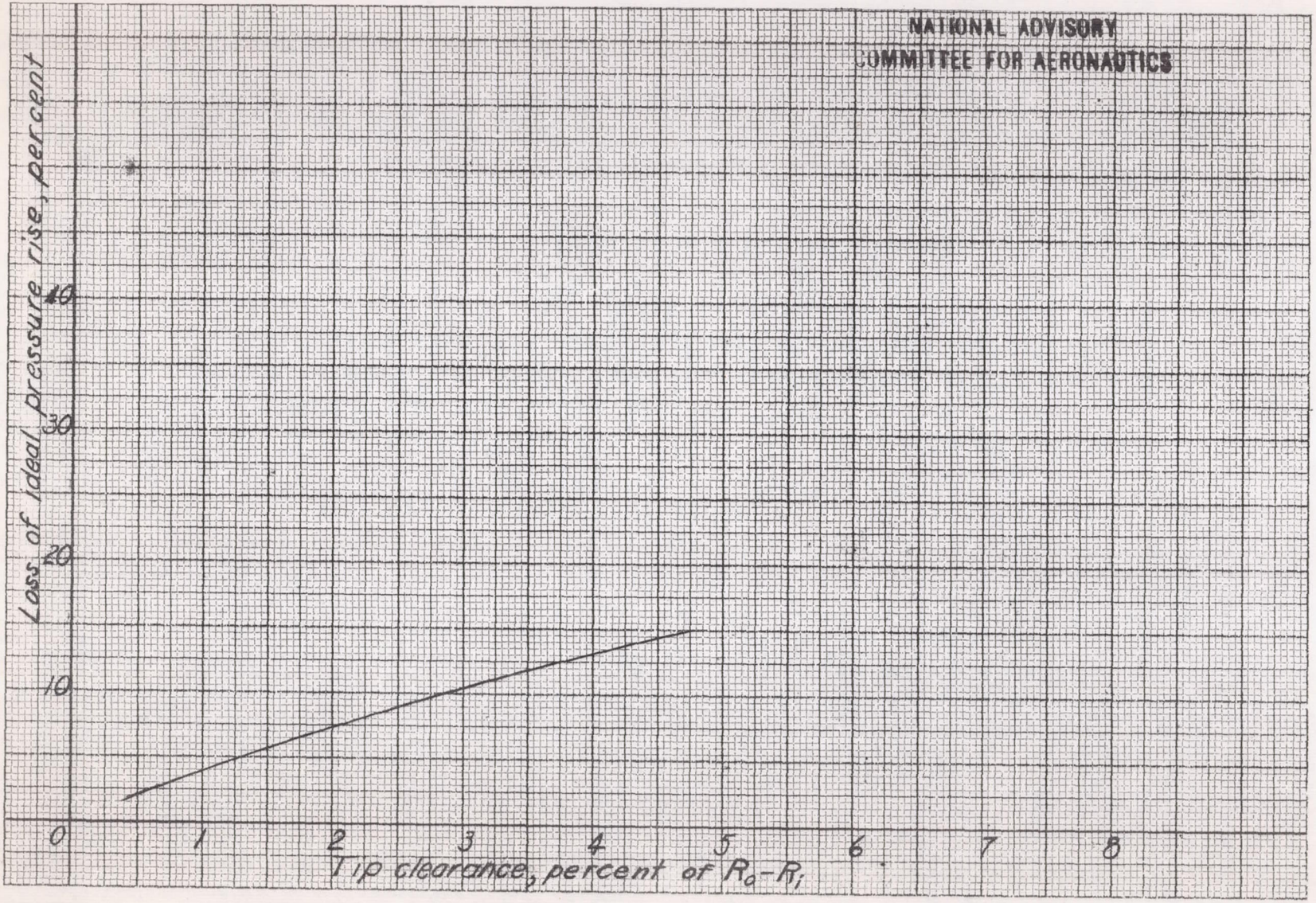

Figure 3.- Tip-clearance losses in percent of ideal pressure rise.
(Average of curves taken from reference 2.)

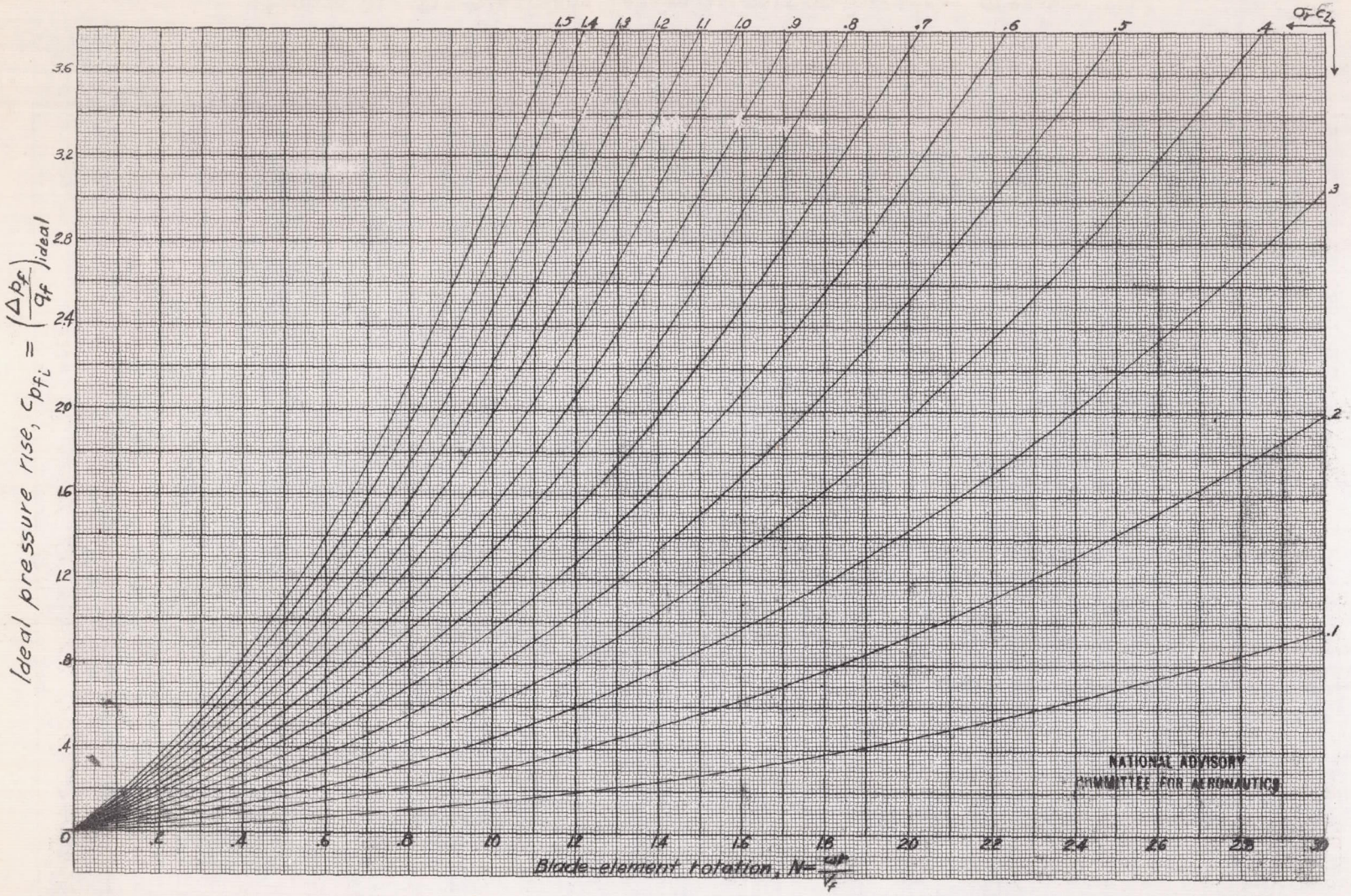

(a) Low N.

Figure 4.- Stator-rotor design chart relating ideal pressure rise, N, and $\sigma_r c_{l_r}$.

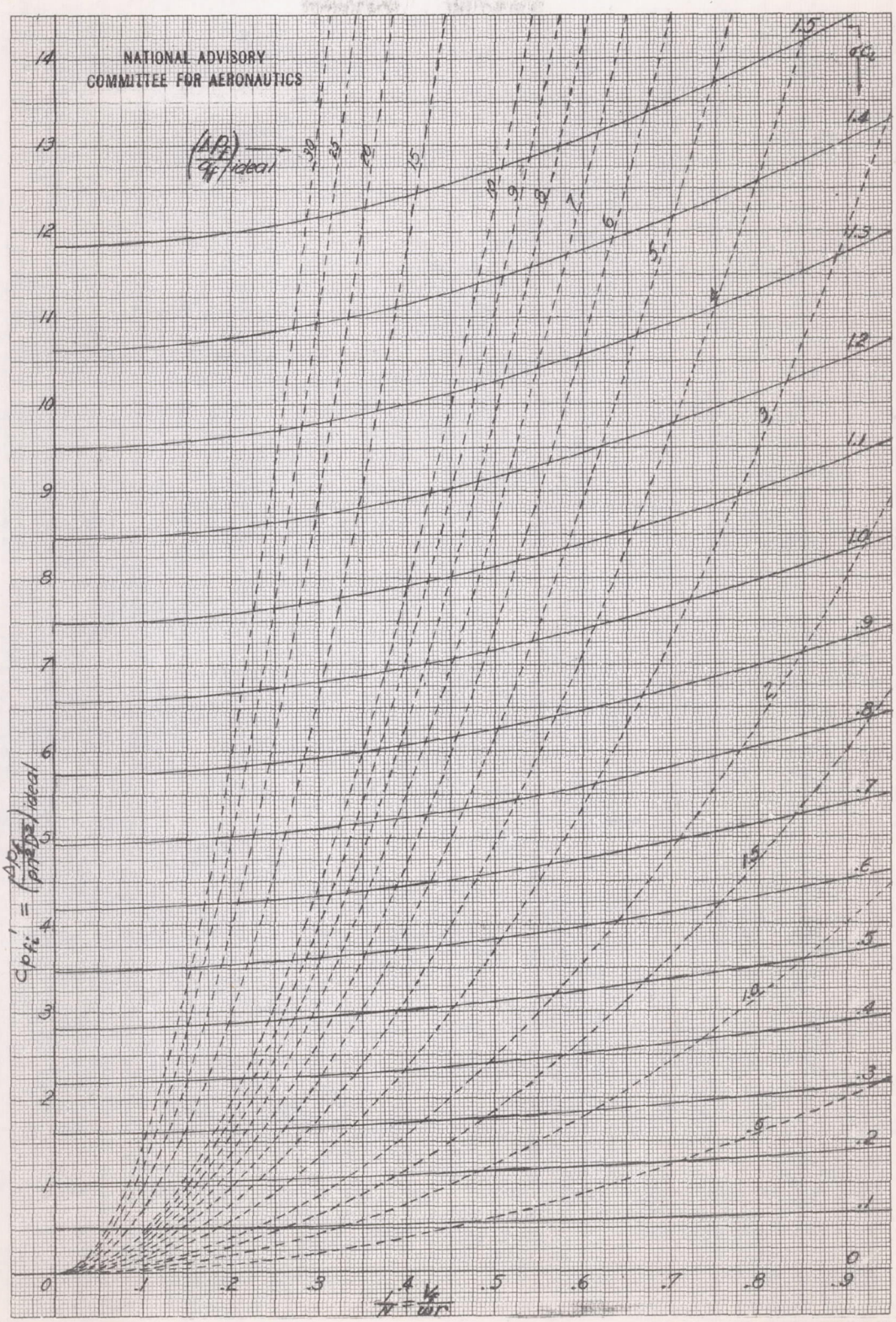

(b) High N.

Figure 4.- Concluded.

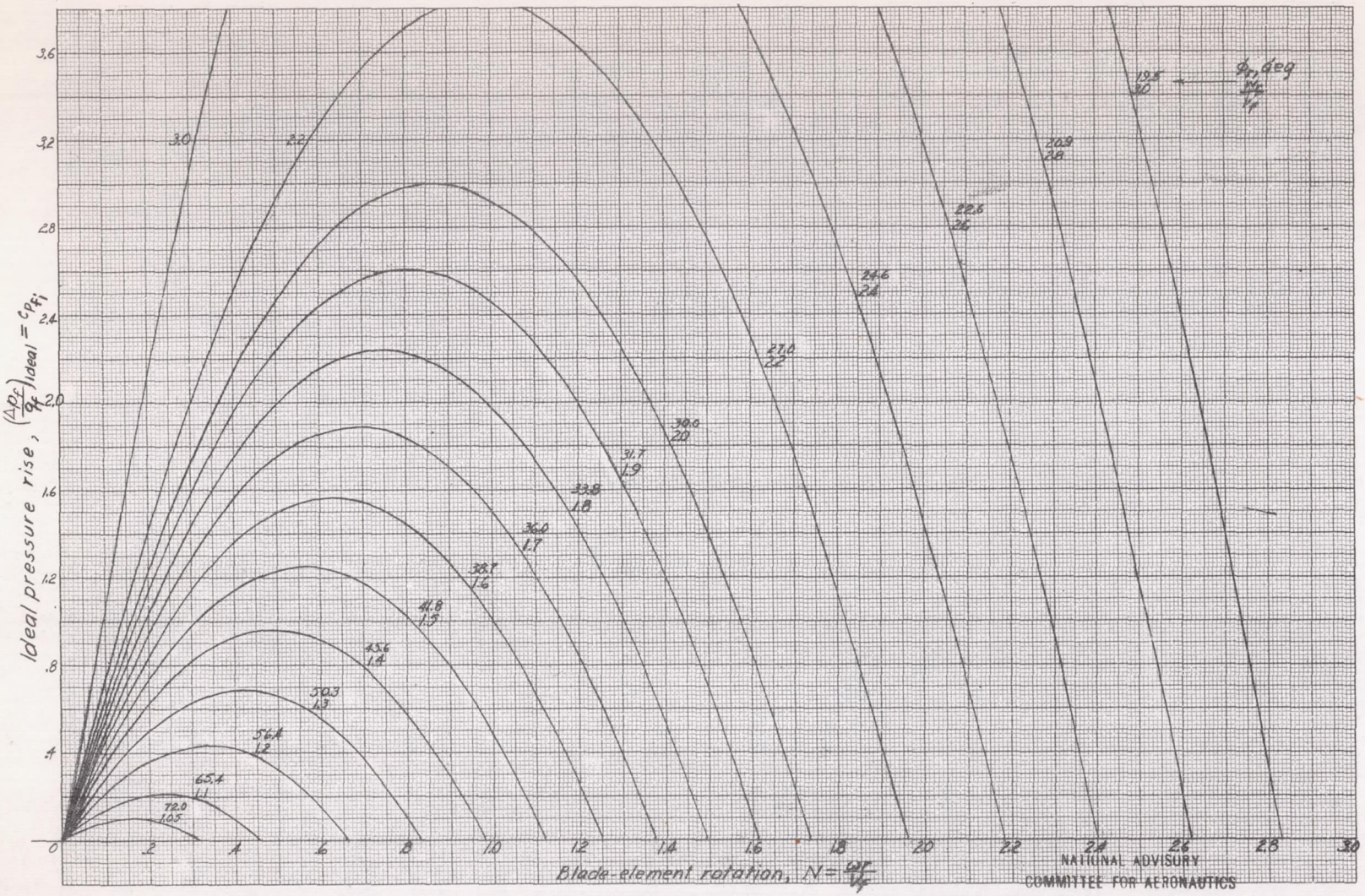

(a) Low N.

Figure 5.- Stator-rotor combination design chart relating ideal pressure rise, N, and w_r/V_f.

L-776

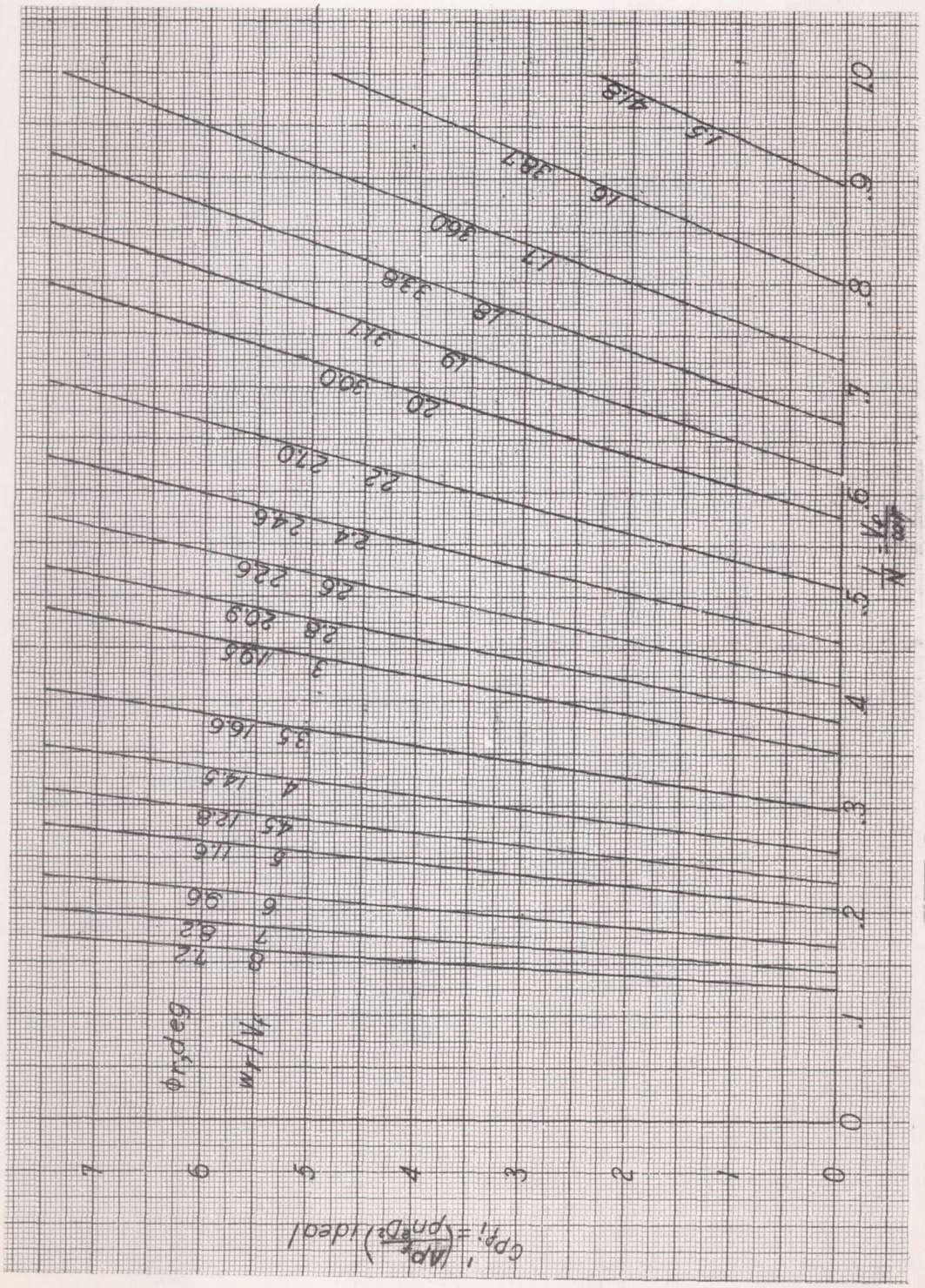

(b) High N.

Figure 5.- Concluded.

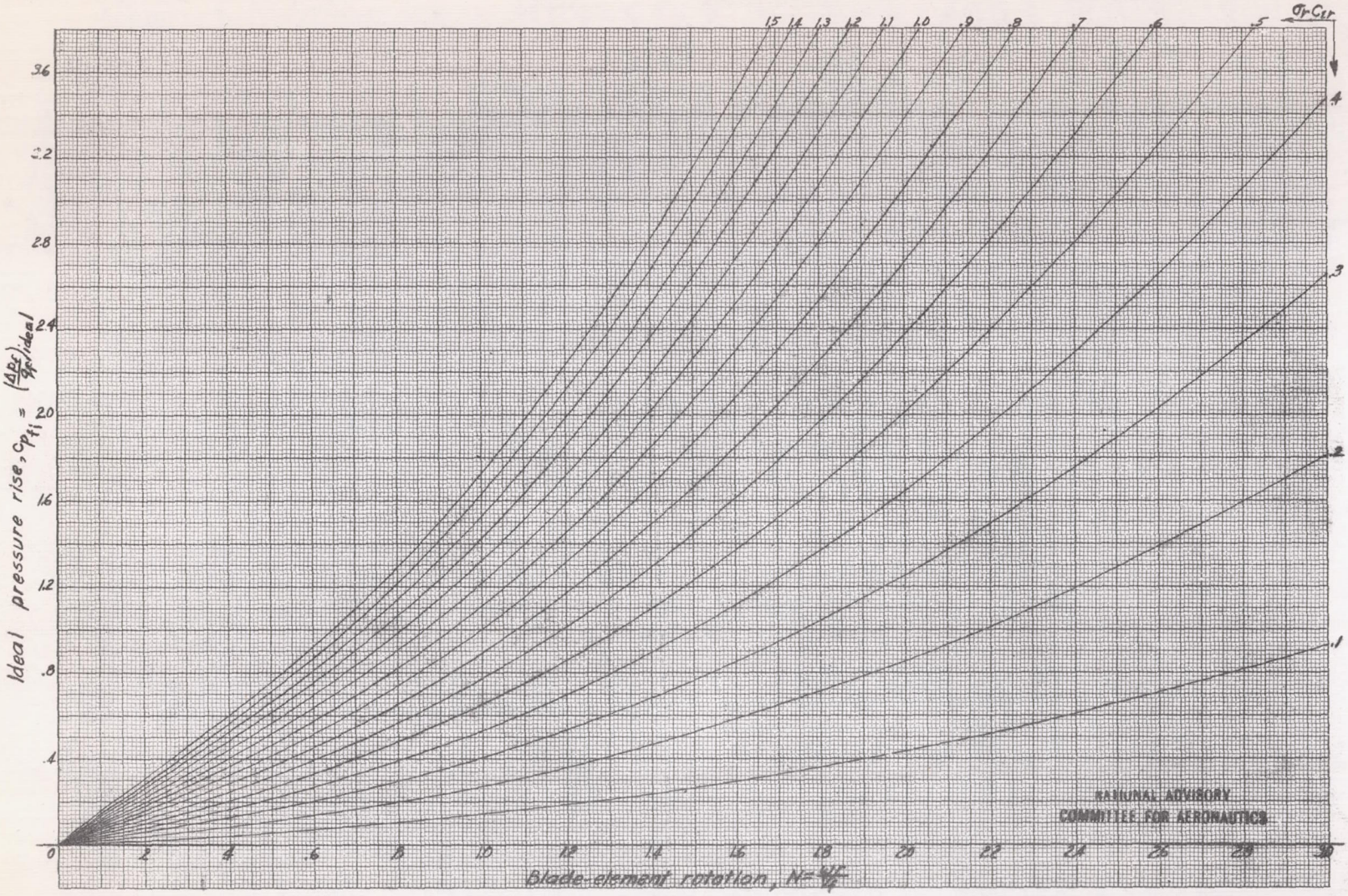

(a) Low N.

Figure 6.- Rotor-stator combination and rotor alone design chart relating ideal pressure rise, N, and $\sigma_r c_{l_r}$.

L-776

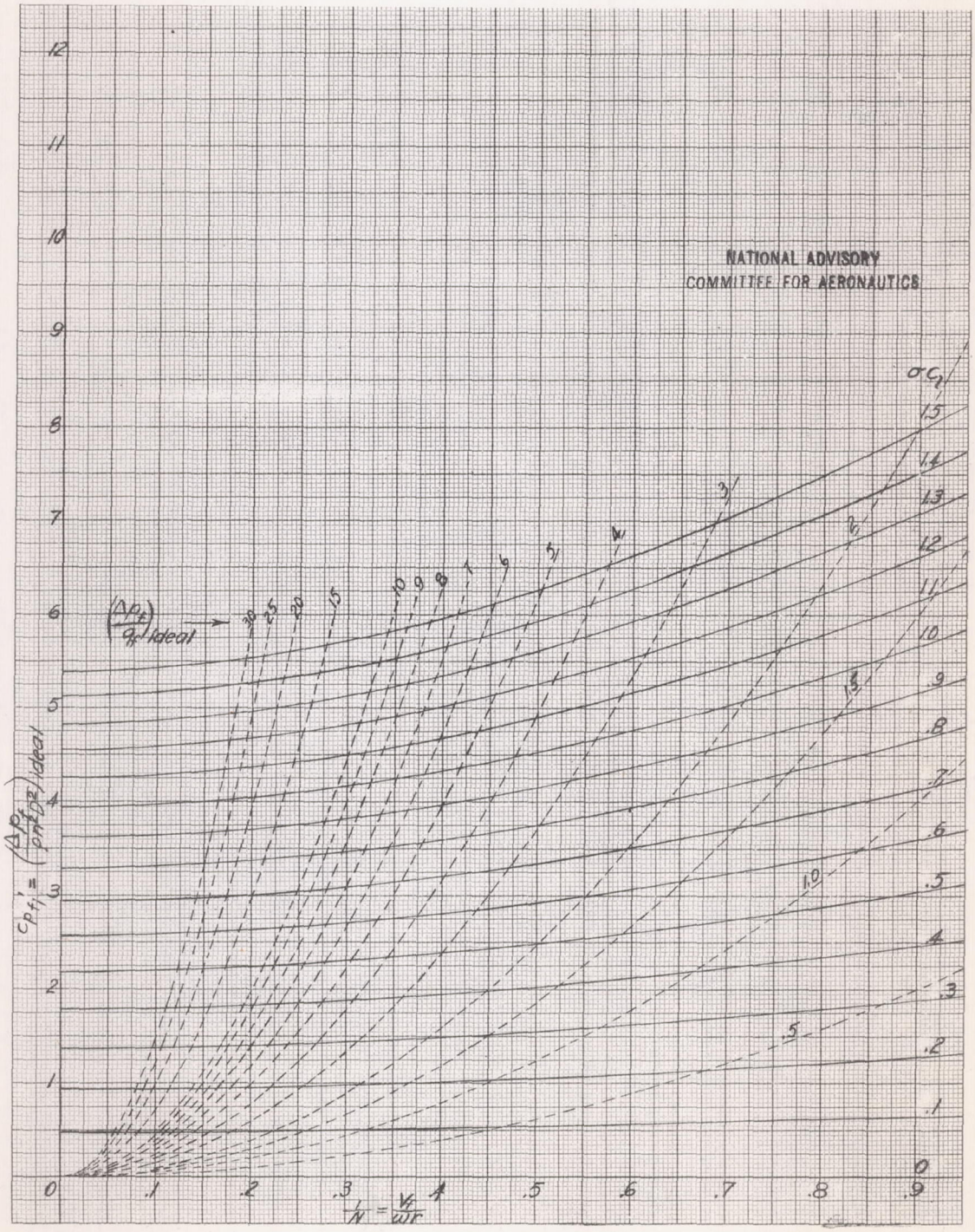

(b) High N.

Figure 6.- Concluded.

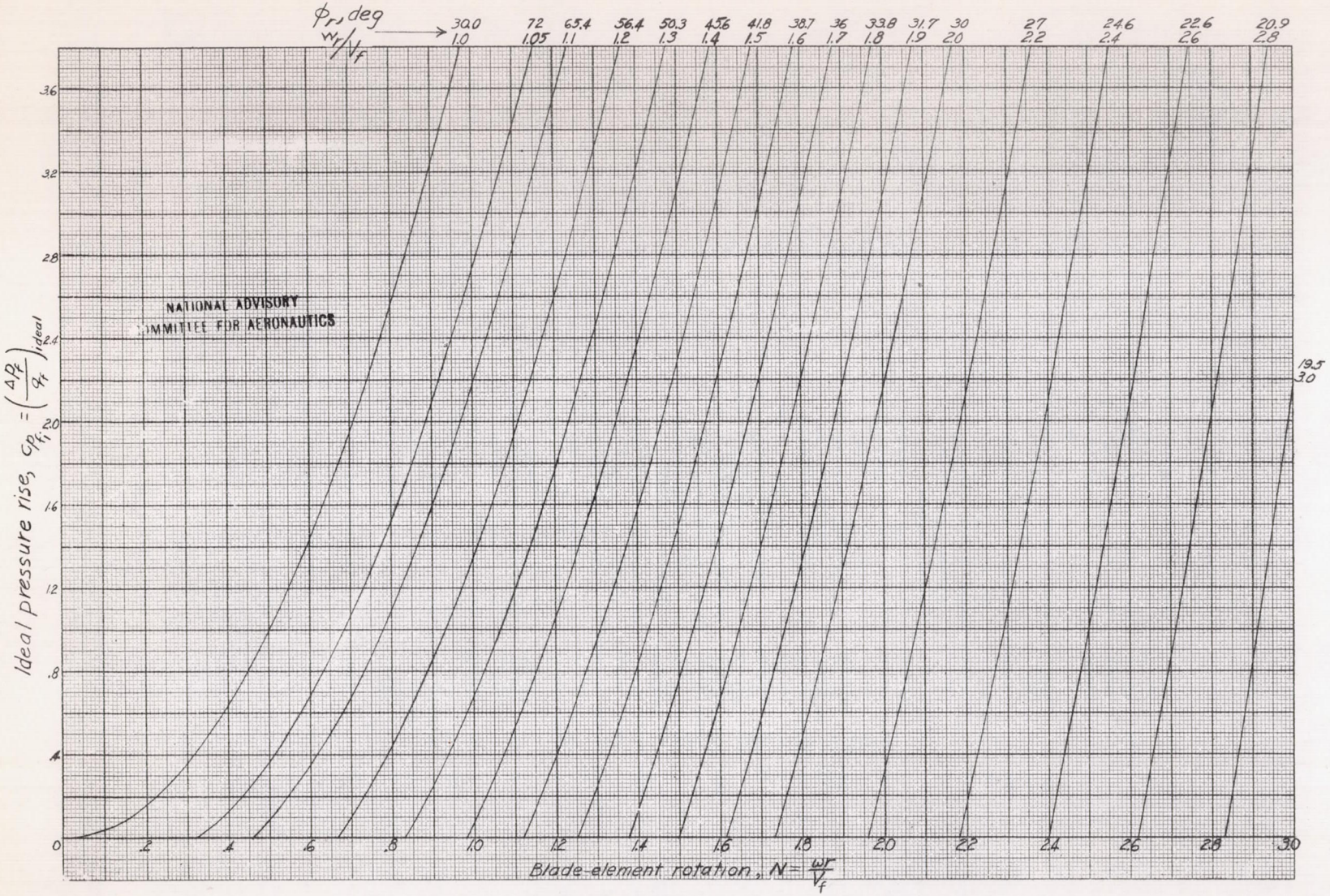

(a) Low N.

Figure 7.- Rotor-stator and rotor-alone design chart relating ideal pressure rise, N, and w_r/V_f.

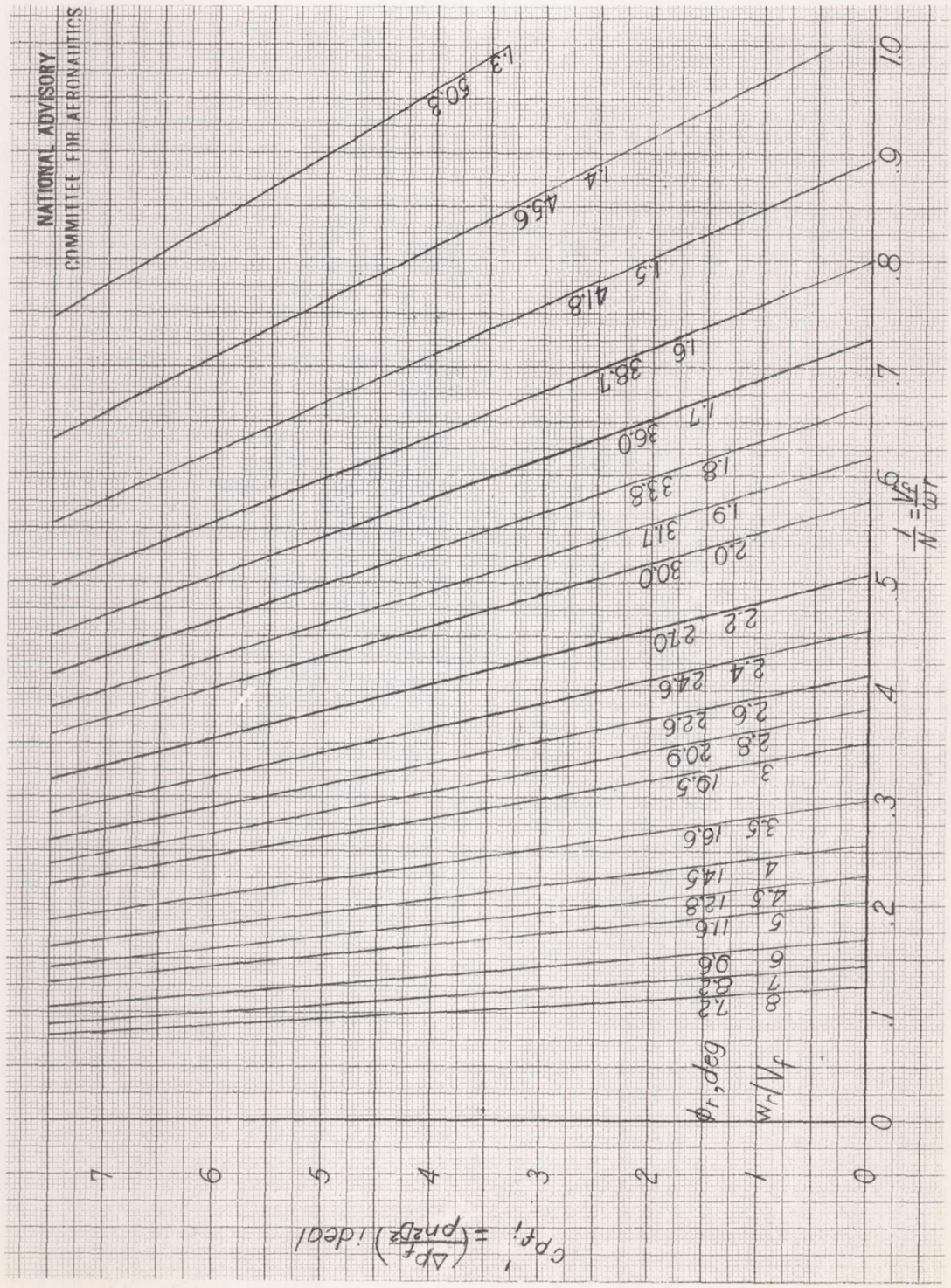

(b) High N.

Figure 7.- Concluded.

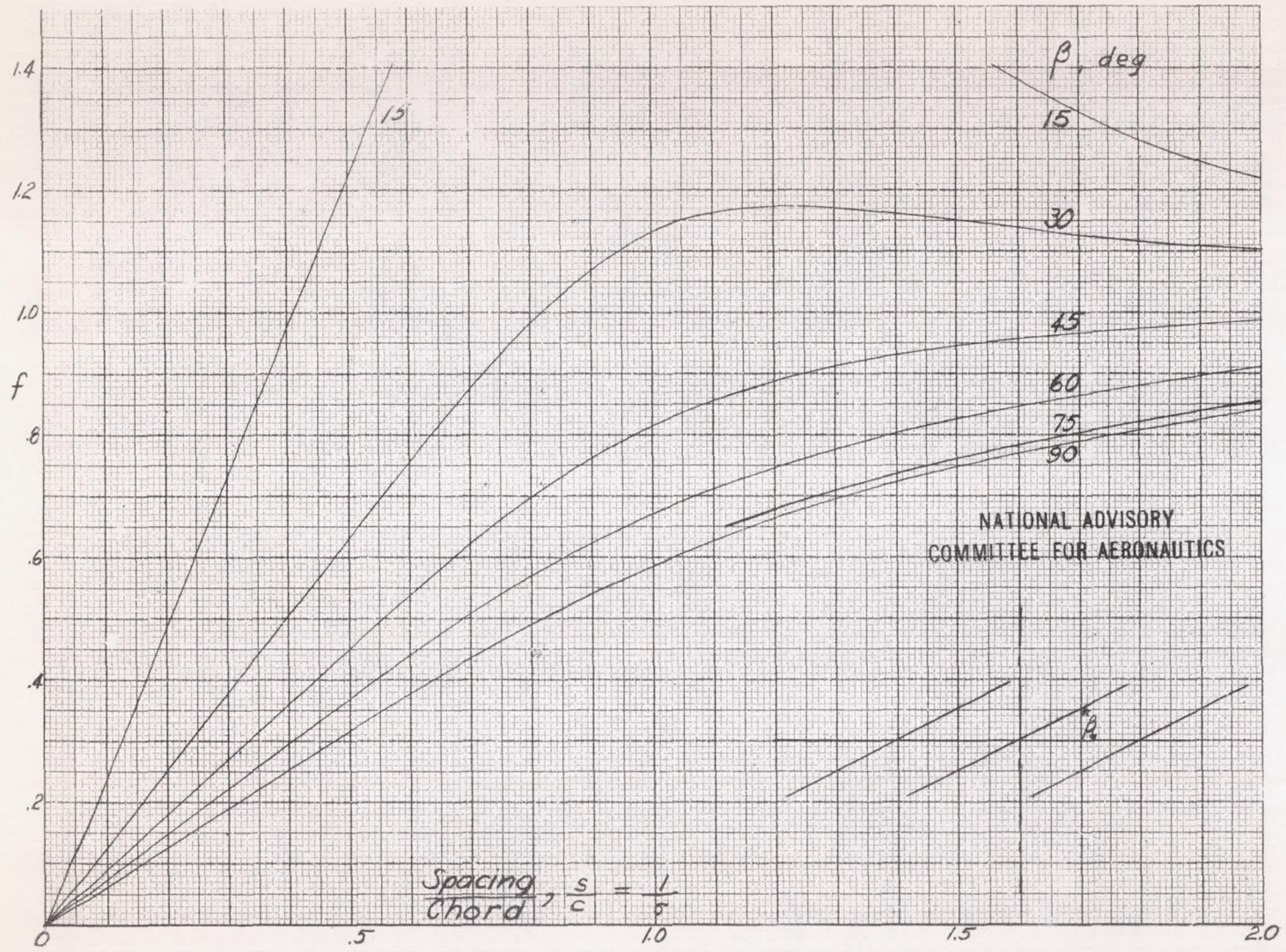

Figure 8.- Cascade lift factor f for high solidity. (From reference 6.)

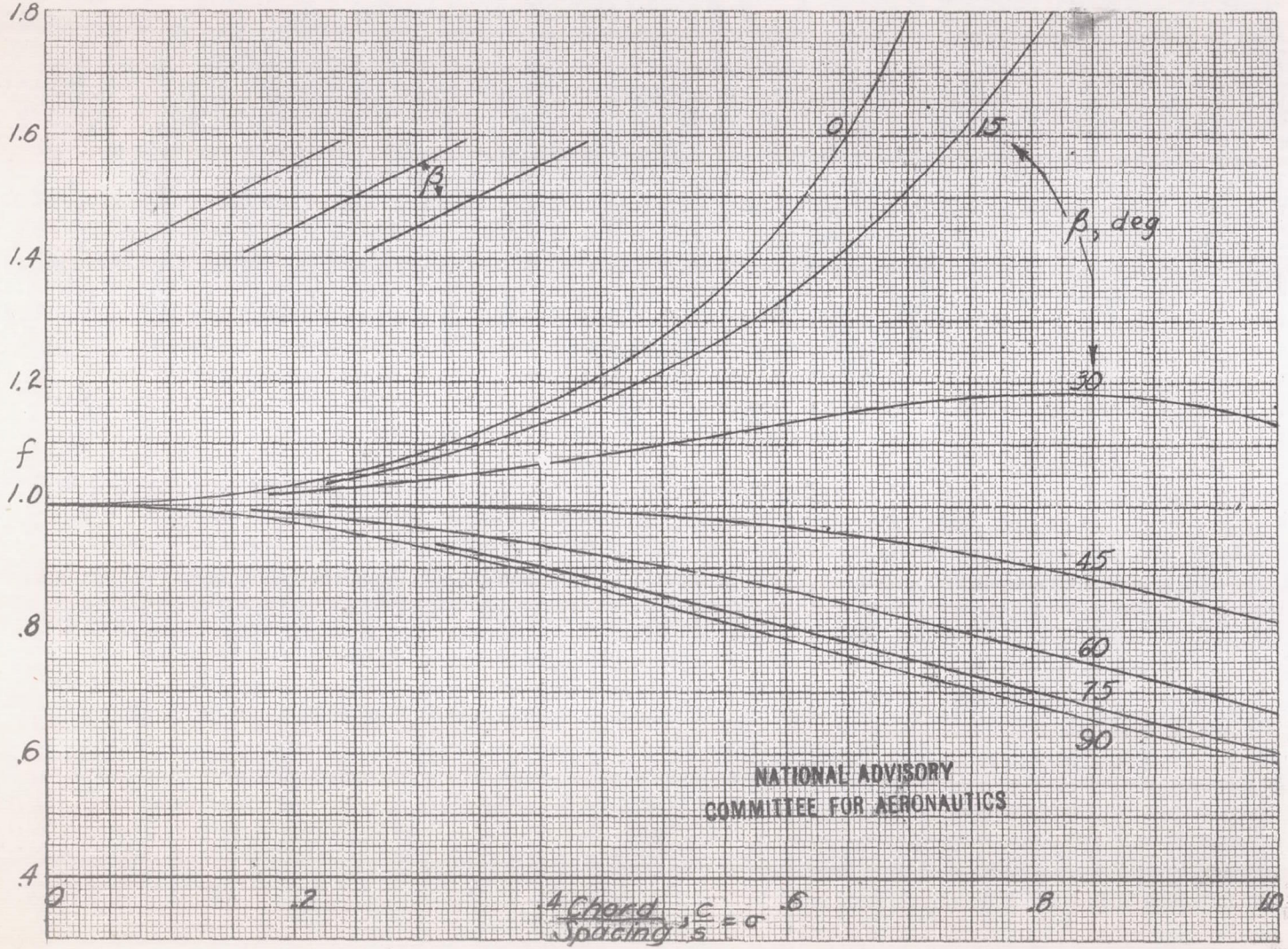

Figure 9.- Cascade lift factor f for low solidity. (From reference 6.)

Figure 10.- Turbine action.

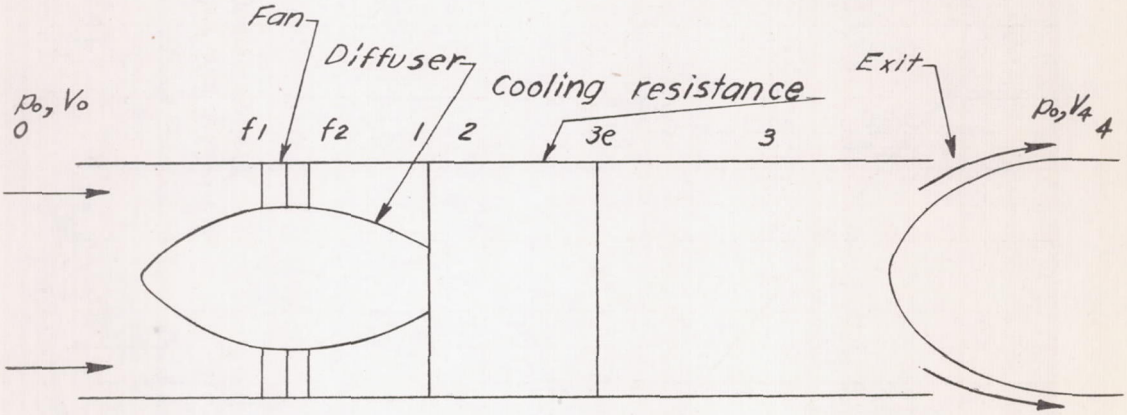

(a) Fan ahead of cooler.

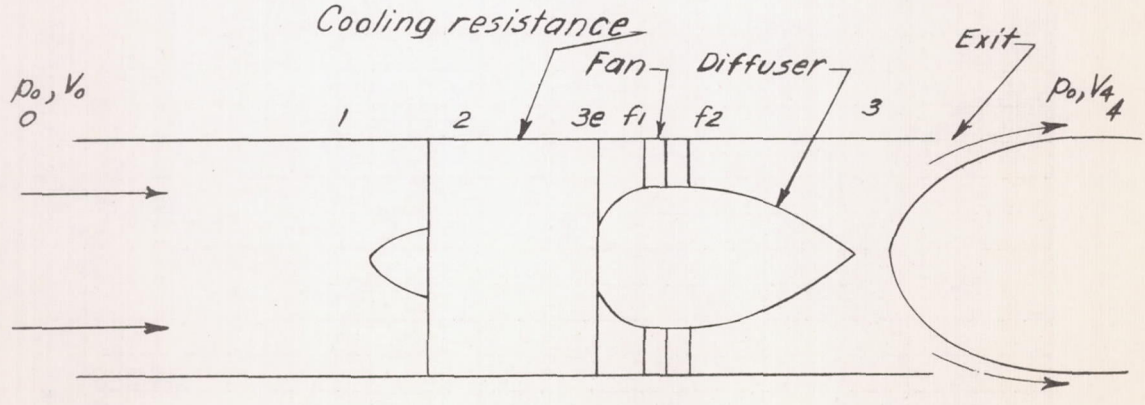

(b) Fan behind cooler.

Figure 11.- Schematic cooling installation.

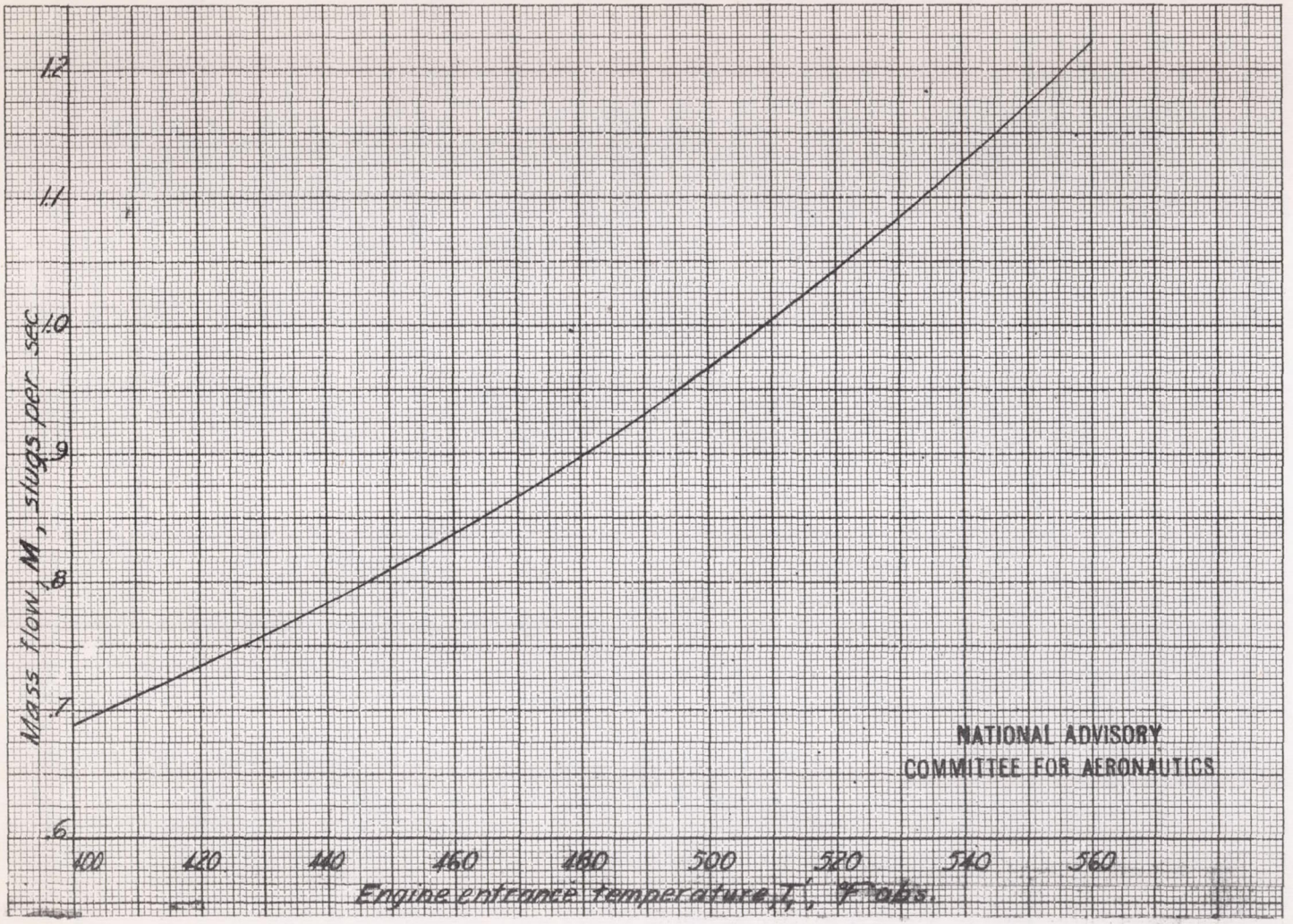

Figure 12.- Assumed mass flow M against air-cooled engine entrance temperature T_1'.

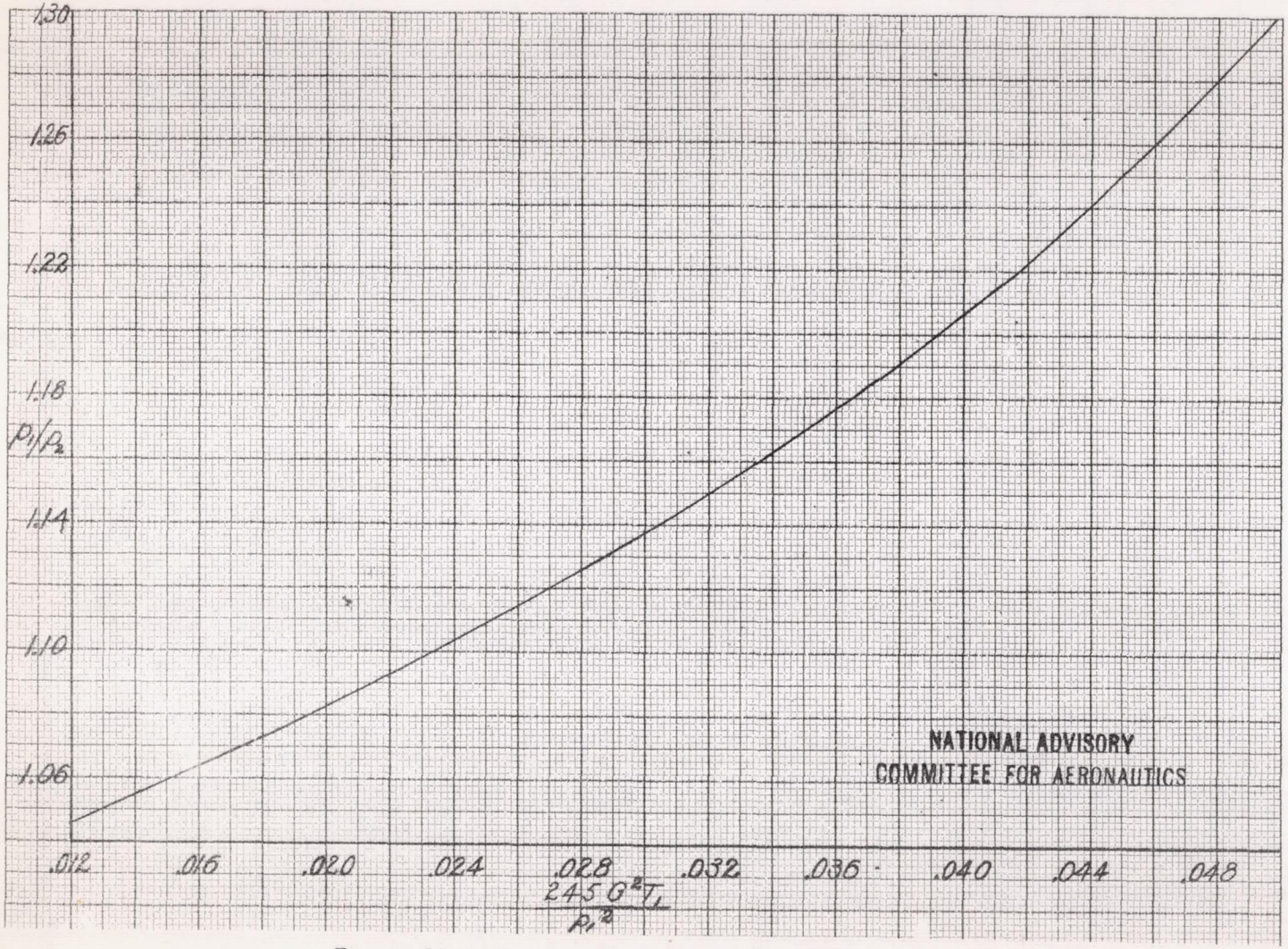

Figure 13.- Graphical solution of equation (52).

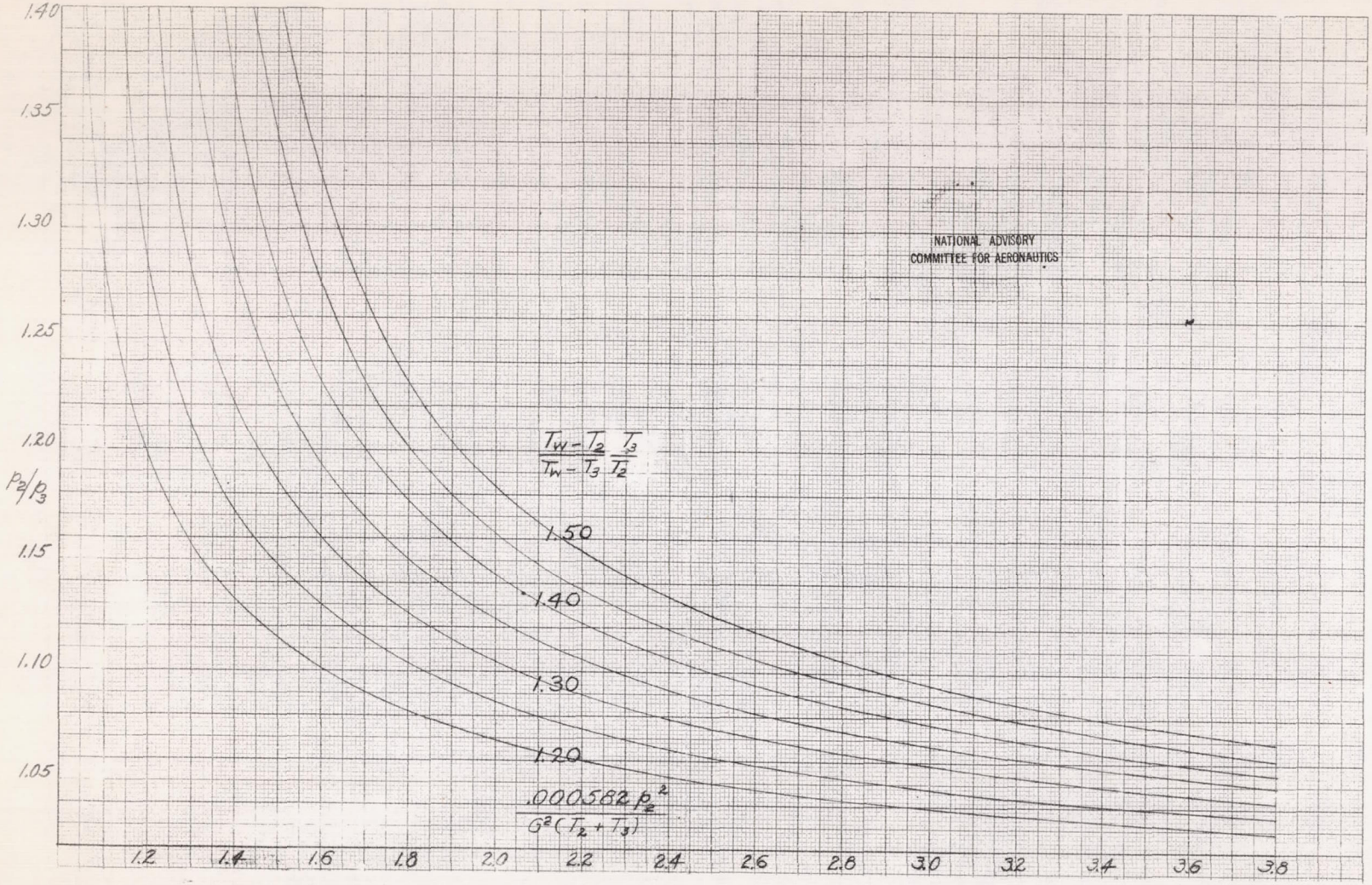

(a) Large values of pressure ratio.

Figure 14.- Graphical solution of equation (53).

L-776

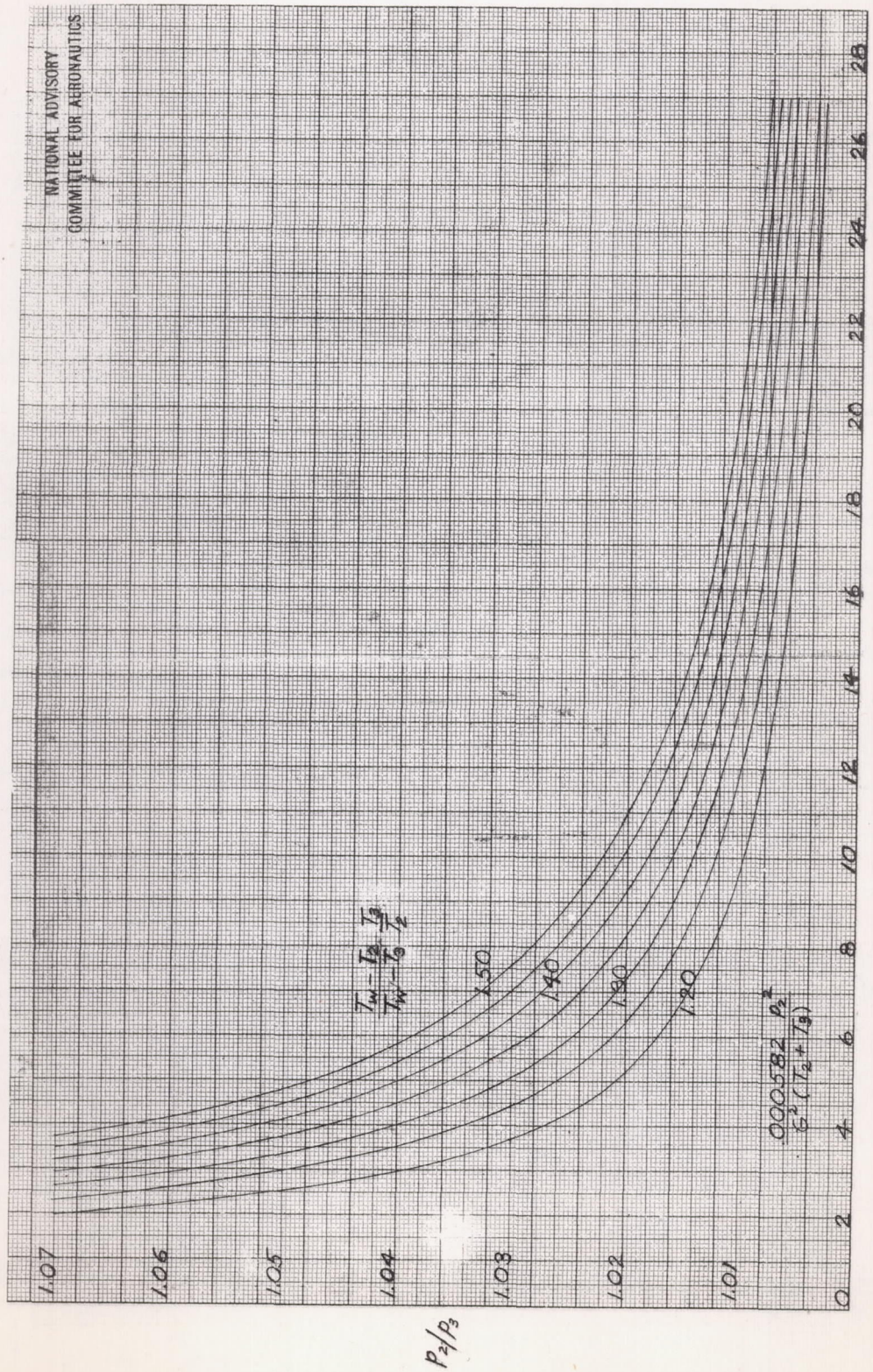

(b) Small values of pressure ratio.

Figure 14.- Concluded.

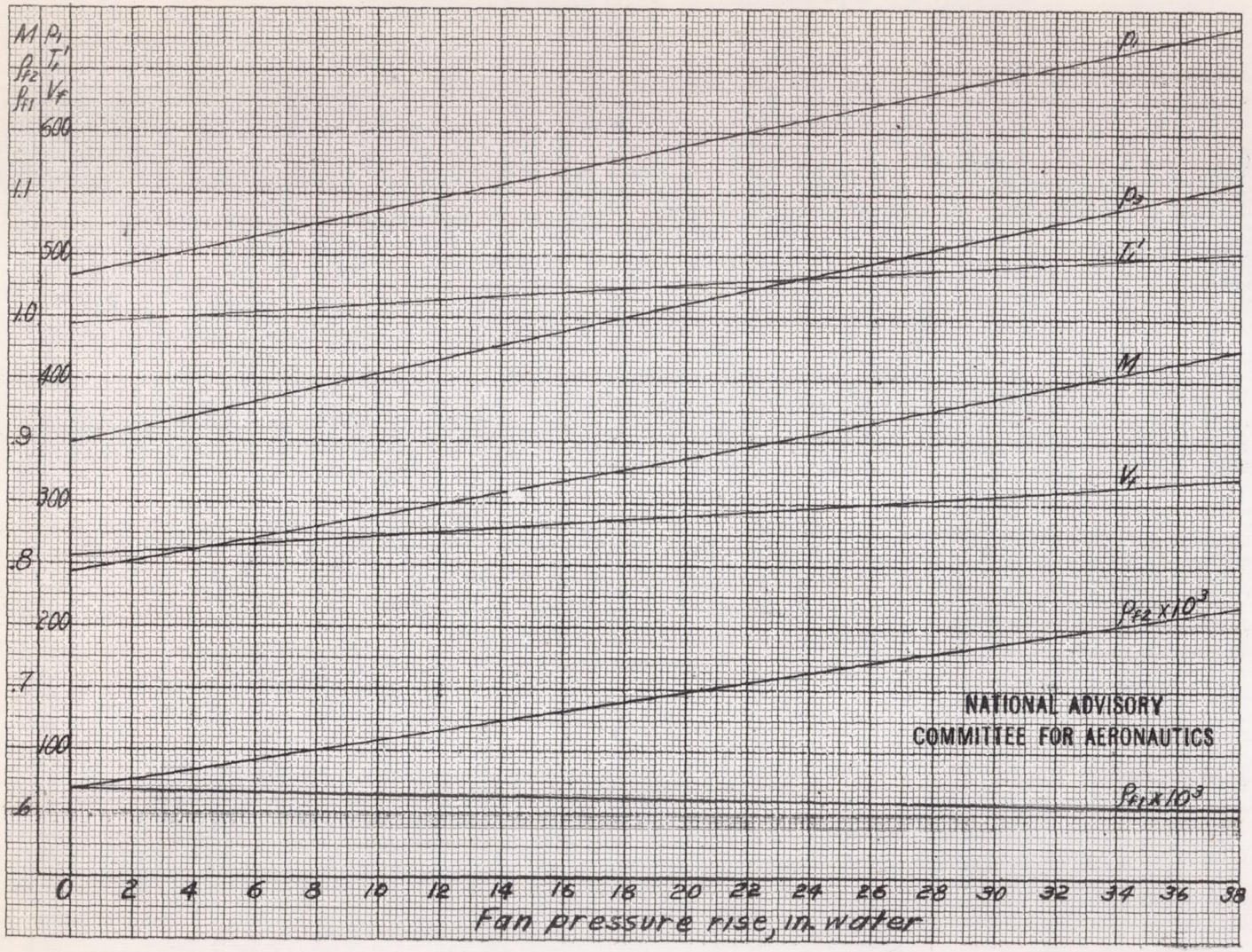

Figure 15.- Cooling-air condition against fan pressure rise.

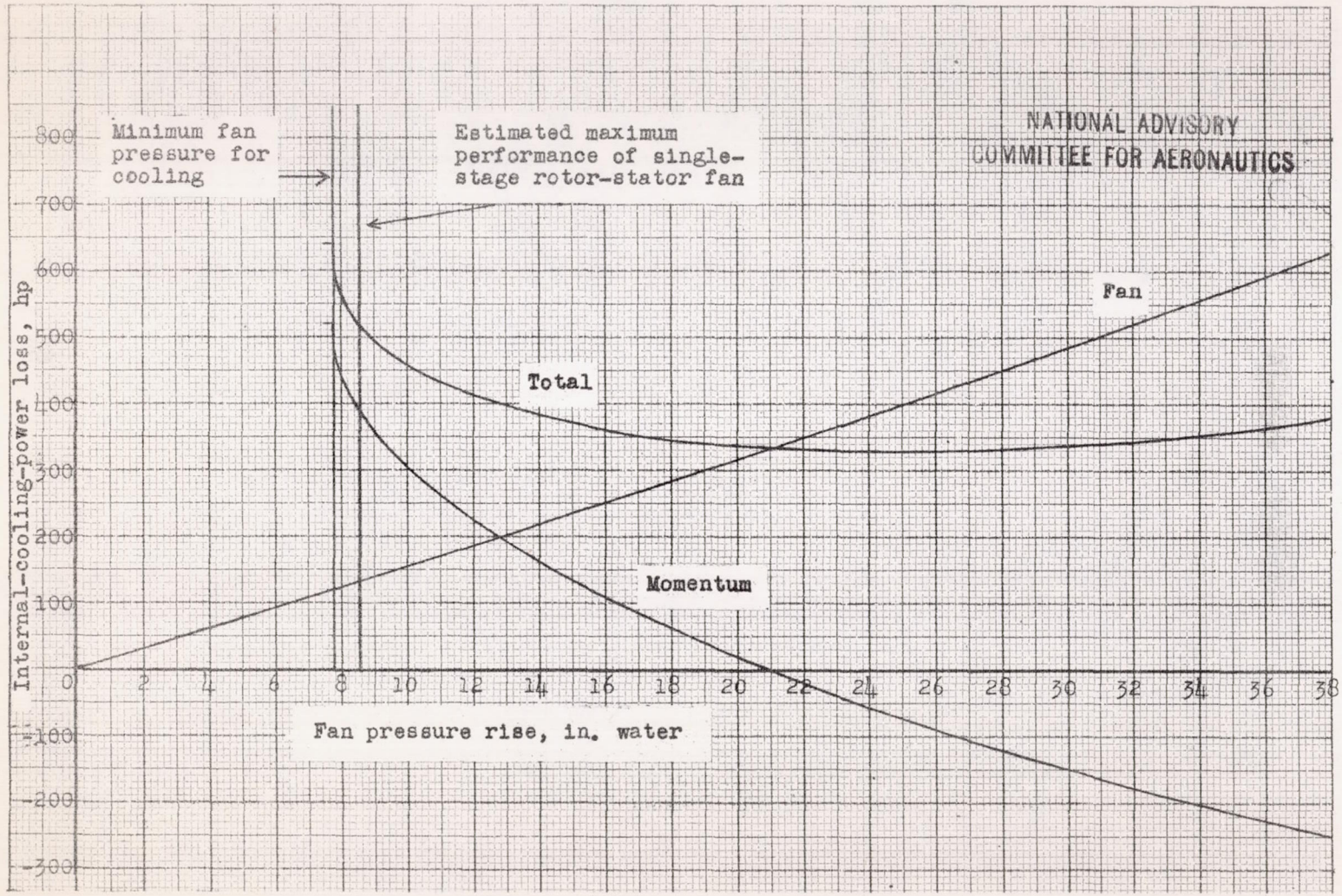

Figure 16.- Internal-cooling-power losses against fan pressure rise.